Modelling the hydrology in the Lake Awassa catchment, Ethiopia

Influences of irrigation and the swamp effect

PM van Dijk

Utrecht University

Front Image: Lake Awassa and its surrounding catchment

(Earthstar Geographics SIO - Microsoft Corporation ©)

Modelling the hydrology in the Lake Awassa catchment, Ethiopia

Influences of irrigation and the swamp effect

MSc Thesis

September 2016

Author: Martijn van Dijk

Student number: 5548195

E-mail: p.m.vandijk@students.uu.nl

First supervisor: Dr. ir. G. Sterk (UU)

Second supervisor: M.F.A. Vogels (UU)

Third supervisor: Kebede W. (HU – WGCF-NR)

MSc Programme: Earth Surface and Water

Faculty of Geosciences

Department of Physical Geography

Utrecht University

Utrecht University

HAWASSA UNIVERSITY

Acknowledgment

First of all, I would like to thank Geert Sterk for all his guidance, advice and the encouragement he has given me. He helped me to give this thesis an interesting, versatile and educational aspect and he helped me to finish my thesis. I want to gratefully thank him. Secondly I want to thank my second assessor Marjolein Vogels for the educative and fun time, especially during the fieldwork in Ethiopia. Her support and guidance was very useful. Furthermore I would thank Kebede Wolka for his support and time in Ethiopia. I cannot forget the support of my friends Bethlehem Abebe, Dong-Gill Kim, Justin Donnelley in Ethiopia. I had a very pleasant time in Ethiopia because of my friend and fellow student Jelle Degen supported and entertained me every day. Finally, I want to thank my family and all my friends that have listened to my enthusiastic words.

Abstract

During the last decades some large changes have taken place in the Main Ethiopian Rift (MER) areas regarding the hydrology. A special case of hydrological changes in one of the MER lakes is lake Awassa. The water balance of Lake Awassa and its catchment area is not well understood. The aim of this study was to quantify the water balance of the Lake Awassa catchment area. This quantification includes the impact of a large swamp (Lake Cheleleka) on the outflow from the catchment and the water withdrawals for irrigation purposes.

The current study used the Soil and Water Assessment Tool (SWAT) to quantify the water balance in the Awassa catchment. It was calibrated and validated using field and observation data from the Tikur Woha and Wosha subbasin. After calibration, model predictions of Tikur Woha streamflow were relatively close to observed values, with a NSE of 0.25 and a R^2 of 0.28. The NSE value of -0.43, during validation period, indicates that the main value of the observed time series would have been a better predictor than the model. According to the PBIAS rating the model performs during both calibration and validation very good. A discharge data set without the backwater effect would very likely result into a better performance overall.

Both streamflow of the Wosha and Tikur Woha river significantly increased during the observed period from 1980 to 1996 and 1981 to 2006 respectively ($p<0.05$). The long-term significant increasing trend of discharge cannot be explained by precipitation changes, since the Awassa and the Wondo Genet observed time series remained constant. The discharge increase of the Wosha and Tikur Woha streams are most likely related to land use changes within the Tikur Woha subbasin, especially to the increase in agricultural land use. The increase in Tikur Woha discharge is very likely smaller than previously stated in other studies due to the backwater effect that significantly affects the discharge measurements.

The irrigation in the Awassa catchments has a medium effect on the total streamflow of the Tikur Woha River. During the dry period the irrigation decreases the streamflow at minimum of -5.8 ± 4.2% in December to a maximum of -13.8 ± 7.7% in February.

The swamp has a significant effect on the water balance in the Tikur Woha subbasin. First of all, the discharge during the wet months increases significantly with values between 100 and 150%. And secondly, all runoff waters located upstream are buffered by the swamp. When the swamp area declines the high peak discharges aren't retained by the swamp anymore. Thus, future cultivation of the swamp area may lead to flooding of high populated downstream area.

List of keywords:

Ethiopia, Awassa catchment, Tikur Woha subbasin, Land use, Hydrology, Water balance, Lake Awassa, Stream flow, Backwater effect, Swamp, Irrigation

Table of Contents

1. Introduction

The Main Ethiopian Rift (MER) is an eastern branch of the East African Rift System (EARS) (Chorowicz, 2005; Macgregor, 2015). In Ethiopia the MER has a great influence on regional and national level; especially on the hydrodynamics. One of the main hydrological characteristics of the Central and Southern MER region is a chain of lakes, which formed at volcano-tectonic depressions (Ayenew et al., 2007; Hengsdijk and Jansen, 2006; Temesgen et al., 2013). These lakes and their catchment areas provide many ecosystem services (Reynolds et al., 2010). People living in these MER catchment areas are dependent on these lakes for water supply, transport, food production, commercial fish farming, waste disposal, soda ash harvesting, recreation, and tourism (Ayenew, 2004; Ayenew, 2007; Hassan and Jin, 2014).

During the last decades some large changes have taken place in the MER areas regarding the hydrology. The largest changes are indirectly attributed to population growth and directly to land use change; mostly deforestation (Alemayehu Abiye, 2008; Ayenew, 2004; Ayenew, 2007; Ayenew and Gebreegziabher, 2006; Dessie and Kleman, 2007; Hengsdijk and Jansen, 2006; Reynolds et al., 2010; Temesgen et al., 2013). Increased runoff due to deforestation and abstraction of water for irrigation and soda harvesting changed the MER lake levels dramatically over the last three decades (Ayenew, 2004; Ayenew, 2007; Hassan and Jin, 2014; Hengsdijk and Jansen, 2006; Temesgen et al., 2013). For example, the level of Lake Abiyata dropped by about 5m (Ayenew, 2004; Hengsdijk and Jansen, 2006; Temesgen et al., 2013), while increased groundwater inputs from percolated irrigation water caused expansion of Lake Beseka (Ayenew, 2004). Such hydrological changes can have important consequences for the people and the environment in the surrounding areas. A better understanding of the MER lakes and their hydrological characteristics can help the local people in making decisions about irrigation systems for agriculture, flood protection, endemic species protection and livestock keeping.

A special case of hydrological changes in the MER lakes is Lake Awassa. The water level of this lake has risen due to a complex combination of land use changes, changes in micro-climate and neotectonism during the last three decades (Achamyeleh, 2003; Alemayehu Abiye, 2008; Ayenew, 2004; Ayenew, 2007; Ayenew et al., 2007; Ayenew and Gebreegziabher, 2006; Reynolds et al., 2010). The rising lake level has frequently caused damage to the infrastructure in the city Awassa, which is situated directly on the eastern lakefront (Achamyeleh, 2003). A protective dike that has been constructed is being threatened by lake levels that over-top the dike (Achamyeleh, 2003). The catchment of Lake Awassa has only one perennial river that flows into the lake. This river, the Tikur Woha, is fed by water from a large swamp. The swamp was originally a lake but between 1972 and 2007 this Lake Cheleleka disappeared and turned into the current swamp (Ayenew, 2004; Gebreegziabher, 2004; Shewangizaw and Michael, 2010; Belete, 2013). The disappearance is mainly ascribed to siltation of the lake caused by deforestation in the upstream parts of the catchment (Ayenew, 2004; Gebreegziabher, 2004; Ayenew et al., 2007; Shewangizaw and Michael, 2010; Belete, 2013).

Despite these problems in Awassa, the water balance of Lake Awassa and its catchment area is not well understood. Some studies have been published about the hydrology in the Awassa catchment area (Alemayehu Abiye, 2008; Belete, 2013; Žáček V., 2014b; Žáček V., 2014a). Alemayehu Abiye (2008) studied the deep groundwater flow and conducted biological and chemical analyses of the Lake Awassa. The study revealed that the Awassa catchment within the closed caldera is an environmentally fragile area where intensive human activity affects the natural resources. Belete (2013) investigated

causal variables for the Lake Awassa water level variability. In this study a correlation between the water level variability and the occurrences of the El Niño-Southern Oscillation (ENSO) phenomenon was found. It was hypothesized that the long-term increasing water level trend of Lake Awassa is probably linked to increased runoff and sedimentation due to anthropogenic factors.

A few studies used hydrological modelling to quantify the water fluxes in the water balance of Lake Awassa and its catchment (Ayenew and Gebreegziabher, 2006; Ayenew et al., 2008; Gebreegziabher, 2004; Herder, 2013; Shewangizaw and Michael, 2010). Gebreegziabher (2004) developed a simple (spreadsheet) hydrological model for the Awassa catchment based on long-term monthly hydro-meteorological data. This model was used by Ayenew and Gebreegziabher (2006) to obtain an understanding of the Lake Awassa water level changes. They compared simulated lake levels with recorded levels, and obtained a good fit for the years 1981-1999. In contrast, the lake levels did not fit for more recent years. They stated that the misfit could be explained in terms of the combined effects of land-use change and neotectonism. In addition, Ayenew et al. (2008) used the same model to estimate the unknown net groundwater flux by comparing the simulated and recorded lake levels in 2008. This study showed the potential of future groundwater exploration. They stated that development demands a good understanding of the hydrogeological system. Shewangizaw and Michael (2010) modelled the hydrological response of the Lake Awassa catchment in relation to the land cover data of the years 1965 and 1998 and simulated a forecast for the year 2017. The study showed an increase in surface runoff, which hypothetically leads to a raising lake level. A more comprehensive study was performed by Herder (2013). She studied the relation between land use and Lake Awassa hydrology in the years 1986 to 2011. The study showed the effect of land use changes on the hydrology in the Awassa catchment. Extensive deforestation has taken place to create agricultural land. This led to an increase in discharge of the Tikur Woha River.

There are two issues, within the existing hydrological studies of Lake Awassa, which have not been taken into consideration. Firstly, the influence of the current swamp on the hydrological response of the main catchment area should be considered. Hypothetically, the swamp has a major influence on the stream flow in the Tikur Woha subbasin, which is located within the Lake Awassa catchment. It is assumed that stream flow from upstream areas is buffered by the reservoir storage function of the swampy area. On top of that, the swamps surface area is decreasing due to siltation and transition of swamp into agricultural land use (Gebreegziabher, 2004). This trend could have a major impact on the local hydrology and thus on valuable ecosystem services.

During the last decades, irrigation in the Awassa catchment has been introduced and it is now widely used to increase the crop yields. These water abstractions may have a large impact on the hydrology in the Awassa catchment, but the influence of water withdrawals due to crop irrigation on the hydrological system at catchment scale has not been studied so far. Hence, the amount of abstracted water due to irrigation is not known in the Lake Awassa catchment.

The aim of this study was to quantify the water balance of the Lake Awassa catchment area in relation to the current land use. This quantification will include the impact of the swamps storage function on the water flow in the Lake Awassa catchment and the water withdrawals for crop irrigation purposes.

2. Site description

2.1 Location

The study area is located in the southern central part of Ethiopia, about 200 km south of the capital Addis Ababa (Fig. 1). The study area covers the Tikur Woha subbasin, which is one of the few main subbasins of the Awassa catchment. It is located directly at the eastern side of the Awassa Lake. The subbasin is named after the Tikur Woha River. This river is the only perennial river that flows into Lake Awassa. The area of the Tikur Woha subbasin is 670 km^2.

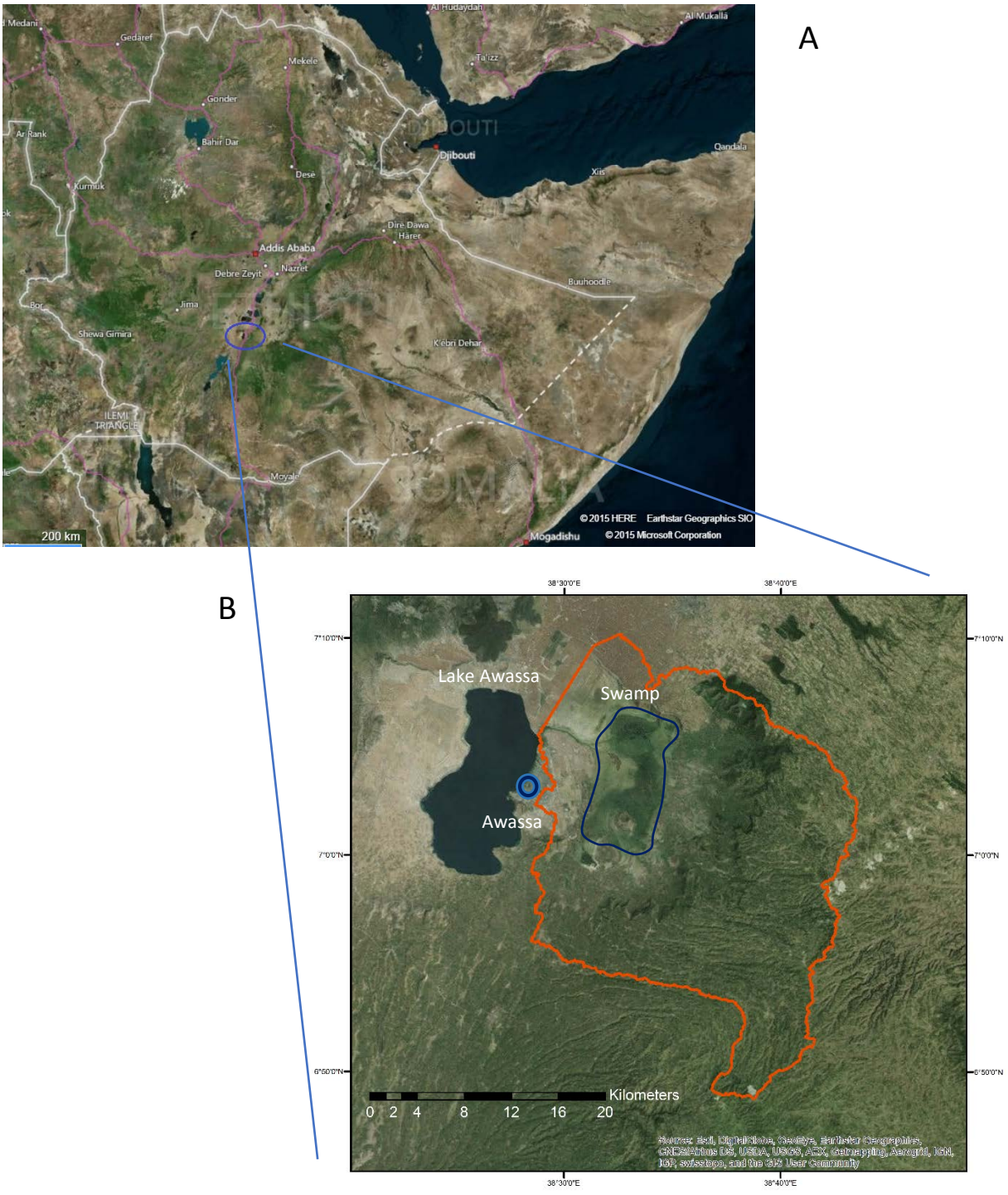

Figure 1: Location of the study area. A: Ethiopia and B: Lake Awassa and the Tikur Woha subbasin (red line).

The Tikur Woha connects the swamp with Lake Awassa (Fig. 1). Eight streams, from which three are perennial, flow from higher grounds to the swamp. The eastern border of the subbasin can be considered to be a small strip of the plateau next to the mountain ridge (caldera rim) east of the village Wondo Genet.

2.2 Geology and Topography

The Awassa catchment has a volcanic origin. It was formed due to intensive tectonic activity. This tectonic activity is a direct result of the Main Ethiopian Rift (MER); the eastern branch of the East African Rift System (EARS) (Chorowicz, 2005; Macgregor, 2015) (Fig. 2). The MER has a NE-SW orientated rift zone.

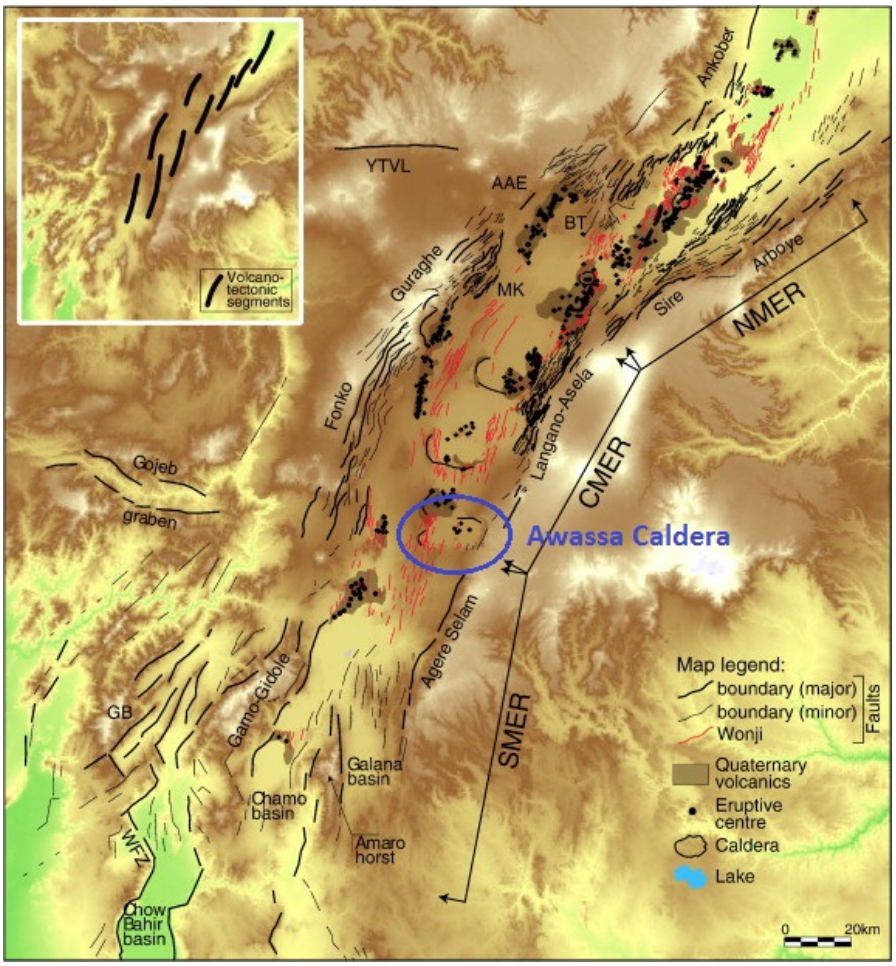

Figure 2: Tectonic sketch map of the Main Ethiopian Rift containing the Awassa Caldera superimposed on a digital elevation model. Modified from Corti (2009).

During Miocene age some volcanic eruptions formed a collapsed caldera with a depression in the center (Alemayehu Abiye, 2008; Ayenew, 2007; Corti, 2009). Lake Awassa was formed at the center in one of the collapsed calderas in the MER. The lake can be considered as a closed system lake (Ayenew et al., 2007). The freshwater lake is located 1680 m above sea level. A groundwater outflow from the lake is considered to be the source of the maintained freshness of the lake (Ayenew, 2007). The caldera rim surrounding the Awassa caldera rises up to a maximum of around 2550 m above sea level. The geology of the Awassa area consist of different volcanic deposits such as alkaline and peralkaline rocks (Late Miocene), Basaltic lava flows (Pleistocene to recent), Acidic volcanics (Pleistocene to recent), and

Volcanoclastic lacustrine sediments (Pleistocene to recent) (Alemayehu Abiye, 2008). A few decades ago, Lake Cheleleka was the second lake in the area located about five kilometer to the east of Awassa. This lake was about 11 km long and 6 km wide, but disappeared decades ago (Ayenew, 2004; Hengsdijk and Jansen, 2006; Ayenew, 2007; Dessie and Kleman, 2007). The former Lake Cheleleka is now a swampy area. The swamp reacts as a natural reservoir. Nearby the town Wondo Genet (Fig. 1) and in the northern part of the swamp some geothermal springs can be found, which indicates that the region is still tectonically active (Alemayehu Abiye, 2008; Ayenew et al., 2007).

2.3 Climate

The mountains and high plateaus of Ethiopia greatly influence the climate. In Ethiopia three seasons can be distinguished based upon the distribution of rainfall (Belete, 2013; Bewket and Sterk, 2005; Cheung et al., 2008; Seleshi and Zanke, 2004). The distribution of rainfall in 5 different rain gauge areas is plotted in figure 3. The locations of the rain gauges are presented in Appendix 8.1: Locations of weather stations. The precipitation in the southern plateau region (Waterersa) is higher compared to the region in the in the North (Shashemene). The three seasons can be distinguished in all five regions.

The first season is the main rainy season ranging from June to September. This season is locally called the *Kiremt*. The northward migration of the intertropical convergence zone (ITCZ) is one of the causes for the precipitation during the *Kiremt* in Ethiopia. In addition, development of the tropical easterly jet and high-pressure systems over the South Atlantic and South Indian Oceans provides precipitation over Ethiopia (Seleshi and Zanke, 2004). In August, in the *Kiremt,* the annual mean maximum monthly precipitation is 119.8 mm in the Awassa Catchment (Alemayehu Abiye, 2008).

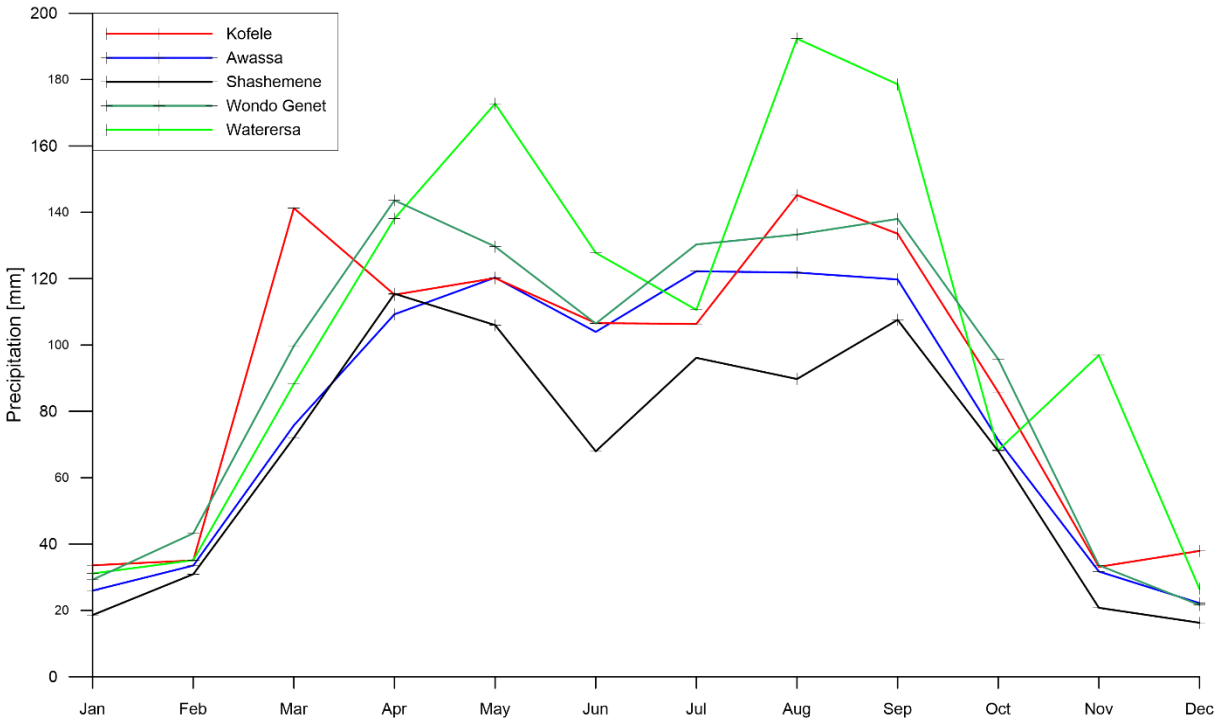

Figure 3: Average monthly precipitation of rain gauges located in or just outside the Tikur Woha basin for periods between 1980 and 2014.

The *Bega* is a dry period in most parts of the country. This period last from October to December/January. In this period warm and cool northeasterly winds cross Ethiopia. These winds are predominantly dry winds but can occasionally transport moist air from migratory low-pressure systems originating in the Mediterranean (Seleshi and Zanke, 2004). The annual mean minimum monthly precipitation in the Awassa Catchment is 17.8 mm and occurs in December (Alemayehu Abiye, 2008).

The third season is a minor wet period locally called *Belg*. This season last from February/March to May. The interaction between the Arabian high and Indian high with the development of thermal lows, more to the south, causes (south)easterly winds which cross southern and central Ethiopia. These moist winds are the main cause of the wet period (Seleshi and Zanke, 2004). The oscillation of the ITCZ varies annually.

Furthermore other climatic events like the occurrence of El Niño and La Niña affects the climate since the rainfall in Ethiopia is related to the El Niño–Southern Oscillation index. During El Niño below-average precipitation in the *Kiremt* period is received (Seleshi and Zanke, 2004). In contrast, during La Niña the mean monthly *Kiremt* rainfalls seem to be increased (Korecha and Barnston, 2007; Abtew et al., 2009). Generally the mean annual precipitation in the Awassa Catchment is between 800 and 1200 mm mainly depending on the oscillation of the ITCZ and El Niño–Southern Oscillation index. The temperature ranges from around 12°C in the *Kiremt* period to around 27°C in the *Bega* period.

2.4 land use / cover

The natural land cover in the Awassa catchment originates from tropical forests. These forests support a high biodiversity and provide important ecosystem services. Both are threatened due to deforestation. In the last decades the growth in terms of economy, population, urbanization and most important, agriculture has resulted in large scale deforestation. In the period 1972 to 2000 the natural tropical forest declined from 16% to 2.8% at the southern MER area of Ethiopia (Dessie and Kleman, 2007). The current dominant species are the *Juniperus procera*, which can be found on ridges and at higher elevations, and the *Podocarpus falcatus*, which can be found at lower elevations (Dessie and Kleman, 2007). Some trees can be considered as a category between agricultural crop and natural forest. These 15-20 year old plantation species are Silver oak (*Grevillia robusta* A. Cunn.), Patula pine (*Pinus patula* Schiede & Deppe) (Teklay et al., 2006), Eucalyptus (*Eucalyptus globulus*) and Cypress (*Cupressus lusitanica* Carr.) (Teklay et al., 2006; Ashagrie and Zech, 2010).

A variety of crops is being grown on the agricultural plots. The most important crops are maize (*Zea mays L.*), sugarcane (*Saccharum officinarum L.*), coffee (*Coffea arabica* Benth.), 'ensete' (*Ensete ventricosum* Welw.), khat (*Catha edulis* Forsk.) and teff (*Eragrostis tef*) (Teklay et al., 2006). Especially sugarcane, maize and khat are being cultivated in the basin area. In recent years more and more farmers are switching to cultivating khat. Khat is a valuable product for local people and for export purposes. At higher altitudes, at the caldera rim and plateau, farmers cultivate mostly teff, barley (*Hordeum vulgare* L.) and ensete. The agricultural surface area is respectively smaller due to the hilly conditions compared to the basin below. Furthermore grasslands for grazing stock are abundant.

2.5 Irrigation

Since the last two decades, in the Tikur Woha subbasin, especially the area between the swamp and caldera rim, agricultural plots are being irrigated. Crops are irrigated mostly during the *Bega* period. In this dry period farmers irrigate in various ways. In most areas, in-between the agricultural plots, a vast

and dense network of hand dug channels (Fig. 4A) distribute irrigation water that is diverted from the main stream channel (Fig. 4B). Secondly, at the end of the rain season artificial reservoirs are filled with water that will be used for crop irrigation (Fig. 4C). A few farmers have access to modern technology. Furthermore, by using gasoline pumps they irrigate water from natural streams to plots nearby. The last few years more efficient concrete irrigation channels are being built (Fig. 4D).

Figure 4: Different irrigation structures in the Tikur Woha subbasin: A small and dense irrigation network between agricultural plots, B a one meter width irrigation channel diverts water from the Wosha stream to the crops nearby, C artificial reservoir filled with water for irrigation purposes and D this concrete irrigation channel is built recently.

3. Materials & Methods

In order to quantify the water balance in the Tikur Woha subbasin a hydrological model will be used. The Soil and Water Assessment Tool (SWAT) was chosen to analyze the hydrological flows. The SWAT model was calibrated and validated using measured data from the Tikur Woha subbasin.

3.1 Soil and Water Assessment Tool

The SWAT is a river basin, or catchment, scale model that simulates spatial and temporal physical processes (Arnold et al., 1998; Neitsch et al., 2011). In general, the SWAT model performs quite well and produces satisfying or good results despite a lack of data (Griensven et al., 2012). SWAT was developed at the USDA Agricultural Research Service (ARS) (Arnold et al., 1998). In this study, the latest version of ArcSWAT (2012.10.17) was used in combination with ArcMap (10.2.2). This ArcSWAT version is an ArcGIS-ArcView extension and graphical user input interface for SWAT. SWAT will be described briefly in this section. More detailed information about SWAT can be found in Neitsch et al. (2011).

SWAT can simulate a large number of different physical processes in a catchment. The catchment (or watershed) is generally partitioned into a number of subbasins. Within these subbasins lumped land areas are defined which comprise unique land cover, soil, and management combination. These lumped land areas are defined in the SWAT model as hydrologic response units (HRUs). The hydrology of a catchment can be divided into two sections. The first part is the land phase of the hydrological cycle of the modelled area. The second part is the routing phase of the water within the catchment. In the next paragraph the most important SWAT components will be described briefly.

3.2 Important SWAT components

3.2.1 Hydrology

The basic property of the SWAT model is the catchment water balance. The water balance is a complex combination and interaction between hydrological fluxes such as precipitation, evapotranspiration, surface and groundwater flow (Fig. 5). When these hydrological components are accurately quantified, the SWAT model can be used for quantifying other processes such as erosion, irrigation, plant growth, nutrient cycling, etc. A schematic overview of the water balance is shown in figure 5.

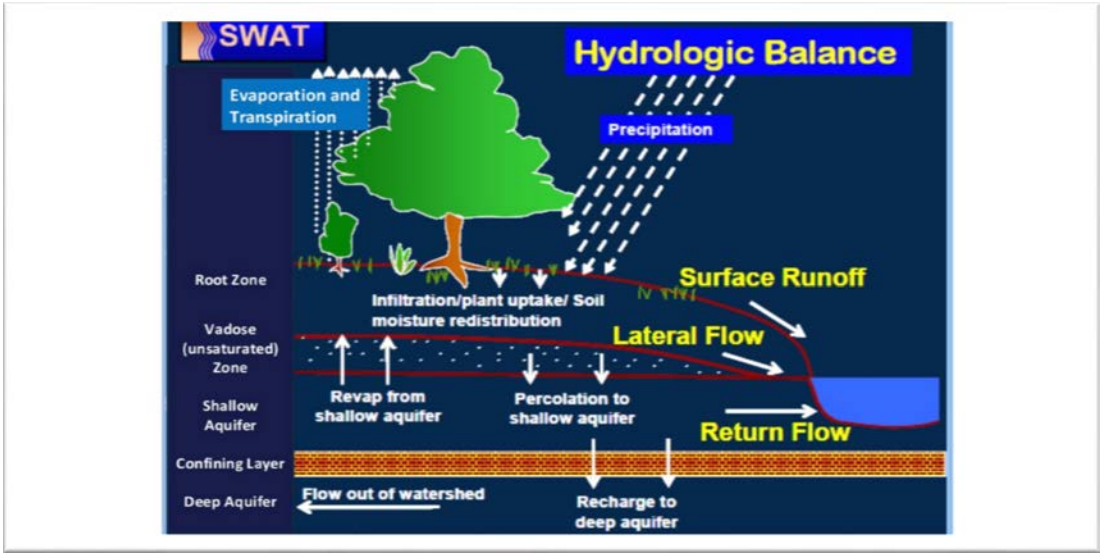

Figure 5: schematic overview of the water balance processes simulated by SWAT (Neitsch et al., 2011), modified by (Zemadim and Schmidt, 2013)

The following water balance equation is used in the SWAT model (Neitsch et al., 2011):

$$SW_t = SW_0 + \sum_{i=1}^{t}(R_{day_i} - Q_{surf_i} - E_{a_i} - W_{seep_i} - Q_{gw_i}) \quad [1]$$

where SW_t is the final soil water content [mm], SW_0 is the initial soil water content [mm], t is the time [days], R_{day_i} is the amount of precipitation on day i [mm], Q_{surf_i} is the amount of surface runoff on day i [mm], E_{a_i} is the amount of evapotranspiration on day i [mm], W_{seep_i} is the amount of percolation and bypass flow exiting the soil profile bottom on day i, and Q_{gw_i} is the amount of groundwater flow into the main channel on day i [mm].

3.2.1.1 Surface runoff

SWAT provides an option to choose between two surface runoff methods. In this study the SCS-Curve Number was chosen to determine the surface runoff since it uses land use information. The SCS-Curve Number empirical model uses the rainfall amount, which can be generated by SWAT or obtained from measured data. The SCS- Curve Number equation is (Neitsch et al., 2011):

$$Q_{surf_i} = \frac{(R_{day_i} - I_{a_i})^2}{(R_{day_i} - I_{a_i} + S_i)} \quad [2]$$

where Q_{surf_i} is the accumulated runoff or rainfall excess [mm], R_{day_i} is the rainfall depth for the day [mm], I_{a_i} is the initial abstractions which includes surface storage, interception and infiltration prior to runoff [mm], and S_i is the retention parameter [mm]. The retention parameter depends only on the CN_i (curve number) for the requested day i.

$$S_i = 25.4\left(\frac{1000}{CN_i} - 10\right) \quad [3]$$

The empirical CN parameter can be calculated by estimating land cover and hydrologic soil groups (HSGs) of an area (Neitsch et al., 2011). The HSGs can be categorized into four groups: A, B, C and D. Group A is defined to have a low runoff potential whereas group D has a high runoff potential. Group B and C have a value in-between. Normally the CN value of all four groups is between 30 and 100.

3.2.1.2 Evapotranspiration

Evapotranspiration is defined as the process that includes evaporation from the plant canopy, vegetation transpiration, sublimation and evaporation from the soil. To estimate the potential evapotranspiration [mm·d^{-1}] several approaches can be used in SWAT (Neitsch et al., 2011). For this study the Penman-Monteith equation was used. The potential evapotranspiration (PET) is a term defined by Penman as the evapotranspiration from a short green crop of uniform height, completely shading the ground and without any water shortages (Penman, 1956). The Penman-Monteith method is an input intensive approach since the method requires air temperature, wind speed, relative humidity and solar radiation.

The Penman-Monteith equation is:

$$\lambda_i \cdot E_i = \frac{\Delta_i \cdot (H_{net_i} - G_i) + \rho_{air} \cdot c_p \cdot \frac{(e_z^0 - e_z)}{r_a}}{\Delta_i + \gamma \cdot \left(1 + \frac{r_c}{r_a}\right)} \quad [4]$$

where λ_i is the latent heat flux [MJ·m^{-2}·d^{-1}], E_i is the evaporation rate [mm·d^{-1}], Δ_i is the slope of the saturation vapour pressure-temperature curve, $\frac{de}{dT}$ [kPa·°C^{-1}], H_{net_i} is the net radiation [MJ·m^{-2}·d^{-1}], G_i is the heat flux [MJ·m^{-2}·d^{-1}], ρ_{air} is the air density [kg·m^{-3}], c_p is the specific heat at constant pressure [MJ·kg^{-1}·°C^{-1}], e_z^0 is the saturation vapor pressure of air at height z [kPa], e_z is the water vapor pressure of air at height z [kPa], γ is the psychrometric constant [kPa·°C^{-1}], r_c is the plant canopy resistance [s·m^{-1}], and r_a is the aerodynamic resistance [s·m^{-1}].

3.2.1.3 Soil Water

Water that infiltrates into the soil first enters the unsaturated zone (Fig. 5). SWAT doesn't simulate the water flow directly. Rather, the simulation is modelled indirectly by using the flux of water that is taken up by plant roots and the flux of water that is evaporated from the soil surface (Neitsch et al., 2011). When the water content exceeds field capacity, water can percolate to the saturated zone. SWAT uses the following equation to calculate the amount of water that percolates to the next layer:

$$w_{perc,ly_i} = SW_{ly,excess_i} \cdot \left(1 - exp\left(\frac{-\Delta t}{TT_{perc}}\right)\right) \quad [5]$$

where w_{perc,ly_i} is the daily amount of water percolating to the underlying soil layer [mm], $SW_{ly,excess_i}$ is the daily drainable water volume in the unsaturated soil [mm], Δt is the length of the used time step [hr], and TT_{perc} is the travel time [hr].

If the soil contains some macropores then water can flow directly as bypass flow towards the saturated zone. SWAT uses the following equation to calculate the amount of bypass flow past the bottom of the profile:

$$w_{crk,btm_i} = 0.5 \cdot crk_i \cdot \left(\frac{crk_{ly=nn_i}}{depth_{ly=nn}}\right) \quad [6]$$

where w_{crk,btm_i} is the amount of water flow past the lower boundary of the soil profile due to cracks in the soil [mm H_2O], crk is the total crack volume for the soil profile on a given day i [mm], $crk_{ly=nm_i}$ is the crack volume for the deepest soil layer $ly = nn$ on a given day i expressed as a depth [mm] and $depth_{ly=nn}$ is the depth of the deepest soil layer $ly = nn$ [mm].

The total amount of water exiting the bottom of the soil profile can be calculated by combining percolation and bypass flow.

$$W_{seep_i} = w_{perc,ly=n_i} + w_{crk,btm_i} \quad [7]$$

where W_{seep_i} is the total amount water exiting the bottom of the soil profile on a given day i [mm H_2O], $w_{perc,ly=n_i}$ is the daily amount of water percolating out of the lowest soil layer n [mm H_2O] and

w_{crk,btm_i} is the amount of water flow past the lower boundary of the soil profile to bypass flow on day i [mm H_2O].

In mountainous areas the percolation of water can result into lateral flow. In SWAT lateral flow is defined as the flow of water that follows a path down a steep hillslope. The water firstly percolates vertically until it encounters an impermeable layer. Directly above the impermeable layer a saturated zone forms. This results into movement of water due to the hillslope. SWAT uses the following equation to calculate the lateral flow (Sloan et al., 1983):

$$Q_{lat_i} = 0.024 \cdot \left(\frac{2 \cdot SW_{ly,excess_i} \cdot K_{sat} \cdot slp}{\varphi_d \cdot L_{hill}} \right) \quad [8]$$

where Q_{lat_i} is the water flux from the hillslope outlet [mm/d], 0.024 the factor needed to convert time [hr > d] and length [mm > m], $SW_{ly,excess_i}$ is the drainable water volume in the saturated zone of the hillslope [mm], K_{sat} is the saturated hydraulic conductivity [mm·hr^{-1}], slp is the increase in elevation per unit distance [m], φ_d is the residual porosity (porosity – porosity at field capacity) [mm·mm^{-1}], L_{hill} is the hillslope length [m].

3.2.1.4 Groundwater

Water from the unsaturated zone can recharge the groundwater in both shallow and deep aquifers. In dry periods water can, due to evaporation from the top layer, flow upwards out of the saturated zone to the overlying unsaturated zone due to capillary forces. In SWAT this process has been named ,, revap''. Water flowing in the shallow aquifer can contribute base flow to a reach within the subbasin. For calculating the groundwater flow that flows into a reach SWAT uses a combined equation of a steady-state equation and a non-steady-state equation (Neitsch et al., 2011).

$$Q_{gw,i} = Q_{gw,i-1} \cdot e^{[-\alpha_{gw} \cdot \Delta t]} + w_{rchrg,sh} \cdot \left(1 - e^{[-\alpha_{gw} \cdot \Delta t]}\right)$$

$$\text{if} \quad aq_{sh} > aq_{shthr,q} \quad [9]$$

$$Q_{gw,i} = 0 \qquad \text{if} \quad aq_{sh} \leq aq_{shthr,q} \quad [10]$$

where Q_{gw_i} is the groundwater flow into the main river/stream in the catchment on day i [mm H_2O], α_{gw} is the baseflow recession constant, Δt is the time step (1 day), $w_{rchrg,sh}$ is the daily amount of recharge entering the shallow aquifer [mm H_2O], aq_{sh} is the amount of water stored in the shallow aquifer on day i [mm H_2O] and $aq_{shthr,q}$ is the threshold water level in the shallow aquifer for groundwater contribution to the main channel to occur [mm H_2O].

In the SWAT model all deep aquifer water is considered to be lost from the system and will not be used for further calculations. The water balance equation that SWAT uses for the deep aquifer system is (Neitsch et al., 2011):

$$aq_{dp,i} = aq_{dp,i-1} + w_{deep_i} - w_{pump,dp_i} \quad [11]$$

where $aq_{dp,i}$ is the amount of water in the deep aquifer on day i [mm], w_{deep_i} is the amount of percolation from the upper aquifer into the deep aquifer on day i [mm], w_{pump,dp_i} is the amount of water removed from the deep aquifer by pumping. It doesn't necessarily have to be artificial pumping

for irrigation or drinking water purposes but it could also be natural movement of water via springs or cracks.

3.2.2 Water routing

3.2.2.1 Channel routing

Main channel processes, like flow routing through the system, can be simulated by SWAT either by the variable storage routing method or the Muskingum routing method (Neitsch et al., 2011). For this study the Muskingum method was used (Overton, 1966):

$$I_t - O_t = \frac{\Delta S_{cs}}{\Delta t} \quad [12]$$

where I is the inflow rate during time t [$m^3 \cdot s^{-1}$], O is the outflow rate during time t [$m^3 \cdot s^{-1}$], S_{cs} is the channel storage [m^3]. The main channel flow and it's flow rate/velocity is simulated with the Manning's equation:

$$v_c = \frac{R_{ch}^{2/3} \cdot slp_{ch}^{1/2}}{n} \quad [13]$$

where v_c is the flow velocity [$m \cdot s^{-1}$], R_{ch} is the hydraulic radius for a given flow depth [m], slp_{ch} is the slope along the water channel [$m \cdot m^{-1}$], n is Manning's roughness coefficient [$s \cdot m^{-1/3}$]. The shape of the channels is assumed by SWAT to be trapezoidal.

3.2.2.2 Impoundment routing

There are two main categories of water bodies that SWAT can model regarding to impoundment routing (Neitsch et al., 2011). Ponds, wetlands, and depressions in the earth's surface are among the first group. These water bodies must be located within a subbasin off the main channel and use their own subbasin for water supply. Water reservoirs are the second group. These are located on the main channel network. The water inflow into the reservoir originates from all upstream subbasins. The water balance equation for a SWAT reservoir can be defined as:

$$V_{t_l} = V_{stored_{t_i}} + V_{in} - V_{out} + V_{pcp} - V_{evap} - V_{seep} \quad [14]$$

where V is the water volume in the reservoir at the last timestep t_l [m^3], V_{stored} is the water volume stored in the reservoir at the first time step t_i [m^3], V_{in} is the water volume flux into the reservoir during Δt [m^3], V_{out} is the water volume flux out of the reservoir during Δt [m^3], V_{pcp} is the volume of precipitation of which falls directly on the reservoir surface during Δt [m^3], V_{evap} is the volume of water that is lost due to evaporation of the reservoir water surface [m^3], V_{seep} is the volume of water that leaves the reservoir due to seepage [m^3].

3.2.3 Crop growth

Crop growth is simulated using the heat unit theory for plant growth. The heat unit theory links a temperature range to plant growth. Growth is limited when there is an occurrence in either water stress, temperature stress, nitrogen or phosphorus stress:

$$y_{reg} = 1 - \max(wstrs_i, tstrs_i, nstrs_i, pstrs_i) \quad [15]$$

where y_{reg} is the plant growth factor (0.0-1.0), $wstrs_i$ is the water stress for a given day, $tstrs_i$ is the temperature stress for a given day expressed as a fraction of optimal plant growth, $nstrs_i$ is the nitrogen stress for a given day, and $pstrs_i$ is the phosphorus stress for a given day.

Management operations that control the plant growth cycle can be addressed for a more accurate land use model. These management operations can consist of a crop harvesting schedule, timing of fertilizer and pesticide and water management operations such as irrigation.

3.2.4 Irrigation

The application of irrigation in SWAT can be set to automatically. The auto-application is triggered by a water stress threshold. Water stress is simulated by comparing actual and potential transpiration:

$$wstrs_i = 1 - \frac{E_{t,act_i}}{E_{t_i}} = 1 - \frac{W_{actualup_i}}{E_{t_i}} \quad [16]$$

where $wstrs_i$ is the water stress for a given day, E_{t,act_i} is the maximum plant transpiration on a given day [mm H_2O], E_{t_i} is the actual amount of transpiration on a given day [mm H_2O] and $W_{actualup_i}$ is the total plant water upatake for the day [mm H_2O]. The water stress threshold has been chosen to be 0.95, which is a threshold value that is being used usually (Neitsch et al., 2011).

SWAT can use different water sources for irrigation such as aquifers, reservoirs, a reach, or a source outside of the modelled catchment. In the study area the source for irrigation is a reach. SWAT diverts the water from a chosen reach to a specified HRU within a chosen subbasin. The amount of irrigation water applied each time when the auto-irrigation is triggered is based on field observations and set to 10 mm.

In SWAT the loss of water due to evaporation or leakages in the conveyance system can be adjusted by an irrigation efficiency factor (Brouwer et al., 1989).

$$e = \frac{e_c \cdot e_a}{100} \quad [17]$$

where e is scheme irrigation efficiency (%), e_c is conveyance efficiency (%), and e_a is field application efficiently (%). A poor irrigation efficiency of 30% has been used.

The loss of water due to evaporation in reaches is calculated by (Neitsch et al., 2011):

$$E_{ch_i} = coef_{ev} \cdot E_{0_i} \cdot L_{ch} \cdot W_i \cdot fr_{\Delta t} \quad [18]$$

where E_{ch} is the daily evaporation from the reach [m^3], $coef_{ev}$ is an evaporation coefficient used for calibrating, E_0 is the potential evaporation [mm], L_{ch} is the channel length [km], W is the channel width at water surface level [m], and $fr_{\Delta t}$ is the fraction of time step in which water is flowing. The water that reaches the soil at the location of irrigation can cause local surface runoff. The surface runoff ratio parameter is set to 0.05%.

3.3 Data collection

Input data is required to run SWAT. A three-months (Sept-Nov 2015) fieldwork in the Tikur Woha subbasin was carried out to collect all required data. This data includes hydrology, meteorology, soil characteristics, land use and land management.

3.3.1 Hydrology

3.3.1.1 Climate

Important input to run SWAT is meteorological data; precipitation and input parameters for the Penman-Monteith potential evapotranspiration method. Five weather stations of the National Meteorological Agency (NMA) are located inside the Tikur Woha subbasin or within a close range of the edge of it (Appendix 8.1: Locations of weather stations). In table 1 the available daily meteorology parameters with their time series are shown. Solar radiation data was taken from the National Centers for Environmental Prediction (NCEP) Climate Forecast System Reanalysis (CFSR) (Dile and Srinivasan, 2014; Fuka et al., 2014). Gaps in measured records were filled by generating climatic data using SWATs build-in program; the Weather Generator. The Weather Generator uses long term statistics of available data. Statistics such as, skew coefficient for daily precipitation in a month, probability of a wet day following a dry day, probability of a wet day following a wet day, average number of days of precipitation in a month have been calculated by the program pcpSTAT (Liersch, 2003a). The program dew02 has been used to calculate the dew point temperature using minimum and maximum daily temperature data (Liersch, 2003b). Furthermore the maximum 0.5 hour rainfall in the entire period of record for a month has been assumed to be 1/3 of maximum daily rainfall in a month (Srinivasan, 2013). Large periods of missing precipitation data was filled manually with the precipitation data of the nearest station provided that it shows similarity.

Table 1: Daily meteorological data obtained by the National Meteorology Agency of Ethiopia (NMA) and Climate Forecast System Reanalysis (CFSR).

Variable	**Weather station**					**CFSR**	
	Awassa	**Kofele**	**Water-ersa**	**Shashe mene**	**Wondo Genet**	**S1cfsr**	**S2cfsr**
Precipitation [mm·day^{-1}]	01/1980-09/2015	07/2000-08/2015	01/2005-07/2015	01/1970 03/2012	05/1977-08/2013	-	-
Relative humidity	01/1980-09/2015	07/2000-08/2015	-	-	-	-	-
Max. temperature [°C]	01/1980-09/2015	07/2000-08/2015	01/2005-07/2015	-	-	-	-
Min. temperature [°C]	01/1980-09/2015	07/2000-08/2015	01/2005-07/2015	-	-	-	-
Solar radiation [MJ·m^{-2}·d^{-1}]	-	-	-	-	-	01/1979-07/2014	01/1979-07/2014
Wind speed [m·s^{-1}]	06/1983-09/2013	07/2000-03/2014	-	-	-	-	-

3.3.1.2 Discharge

Two discharge datasets containing daily discharge data of both Wosha and Tikur Woha steams have been collected by consulting the Ministry of Water, Irrigation & Energy. The Wosha discharge dataset covers a period from 1980 to 1996 whereas the Tikur Woha dataset covers a period from 1981 to 2006. Both localities are located within the Tikur Woha subbasin (8.2 Location flow velocity measurement points).

During the fieldwork period, at the end of the *kiremt*, the discharges of 7 streams have been measured. These are respectively, Wosha, Worka, Hallo, Shonkora, Wedesa, Abosa and the Boga/Galchacha (Appendix 8.2 Location flow velocity measurement points). All 7 streams flow into the swamp. The measurement sites have been chosen in such a way that the flow is not or minimally affected by tributaries and objects such as people, livestock, boulders, holes, logs or thick brushes. Furthermore at most of the measurement sites the stream doesn't meander. A straight section has been chosen because the water flow is likely to be more uniform than near a meander.

Stream flow was calculated by using the Midsection Method (Ahmad et al., 1995; Kuusisto, 1996; Holmes, 2001; Turnipseed and Sauer, 2010; Shedd, 2011):

$$q_x = v_x \left[\frac{b_{(x+1)} - b_{(x-1)}}{2} \right] d_x \qquad [19]$$

where q_x is the discharge through partial section x , v_x is the mean velocity in cell x, b_x is the distance from initial point to vertical x and d_x is the depth of water at vertical x. The Midsection Method is schematic displayed in figure 6.

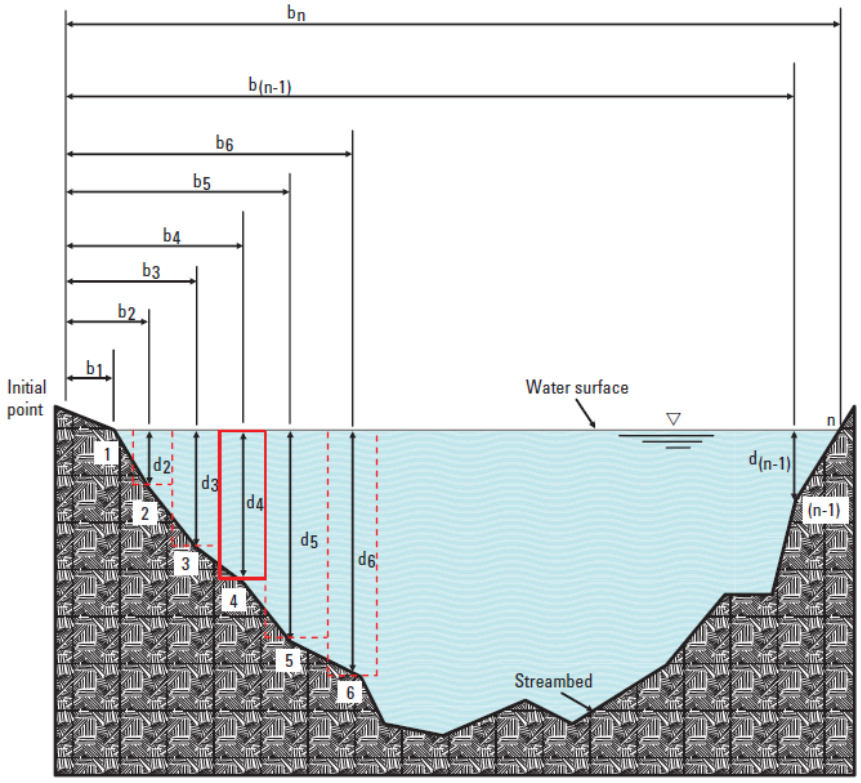

Figure 6: Schematic figure displays the Midsection Method to calculated cross-section area for discharge measurements (Turnipseed and Sauer, 2010)..

In shallow streams the Six-Tenths Depth Method was carried out. This means that the velocity was measured at a water depth of 0.6d below the water surface. The resulting velocity is the mean velocity in the vertical. The mean velocity in a vertical water column is at 0.6d due to a vertical logarithmic velocity distribution profile. The Two Points Method was carried out when the water depth was deeper than ± 50 cm. The velocity was measured at a depth of 0.2d and 0.8d below the water surface. The mean velocity is the average velocity between the two measurement points. This method is more consistent and accurate than the Six-Tenth Depth Method (Ahmad et al., 1995; Kuusisto, 1996; Holmes, 2001; Turnipseed and Sauer, 2010; Shedd, 2011). The velocity was measured by the Aqua Data SENSA RC2 Water Velocity Meter, which uses the Faraday principle of electro-magnetic induction. The probe has a high accuracy of ± 0.5% and can be used in very shallow streams. At all localities the velocity of the water flow has been determined by using the ten seconds auto-averaging option which was performed by the control unit automatically. Each velocity data point has been measured twice. The discharge has been measured eleven times at the location Worka and both upstream and downstream locations of the stream Wosha. Additional, the discharge of the streams Wedesa, Abosa and Boga have been measured three times. At last, the discharge of the streams Shonkora and Hallo have been measured once.

3.3.1.3 Soil type

The Rift Valley Lakes Basin Integrated Resources Development Master Plan Study Project contains a soil map of the Lake Awassa catchment area. Both classification and geographical locations of the soils described by this soil map has been used in the hydrological SWAT model. The major soil types in the Tikur Woha subbasin are Cambisols, Luvisols, Leptosols and Andosols. The Harmonized World Soil Database v1.2 was consulted to collect soil characteristics such as soil texture (Fischer, 2008). Other required characteristics such as available water content, saturated hydraulic conductivity and matric bulk density have been calculated by the SPAW Soil Water Characteristics program (Saxton, 2007). Soil characteristics of the Haplic Cambisol are not available in the Harmonized World Soil Database v1.2. Most Haplic Cambisol soil characteristics are described by Dube et al. (2012). Soil organic carbon content values from the Chromic Cambisols, Chromic Luvisols, Eutric Cambisols, Haplic Luvisols, Vertic Cambisols and Vitric Andosols, measured within the Tikur Woha subbasin (Wolka et al., 2015), have been used instead of the general organic carbon content published in the Harmonized World Soil Database. Organic carbon content can vary spatially due to local weathering, chemical reactions and fertilization.

3.3.1.4 Land use

A land use map was required as input for SWAT. The land use map was created using Landsat Level 1 satellite surface reflectance images. The satellite images were verified during fieldwork. This land use map was developed in a separate Master Research project (Degen, 2016). The land use map has a high spatial resolution (2m). In this study the land use map was slightly modified because the land use map showed some crops within the wetland area. These crops were removed in modified land use map.

The plant characteristics of the crops khat and ensete have been replaced by plant characteristics of coffee and banana respectively due to lack of known parameters. It is assumed that most plant characteristics are not very different than plant characteristics of the crops khat and ensete. However, the optimal- and growth temperature of coffee and banana are modified in order to get a more realistic crop growth.

3.3.2 Water routing

3.3.2.1 DEM

A digital elevation model (DEM) was needed to delineate subbasins connected by water streams in the Awassa catchment. The Advanced Spaceborne Thermal Emission and Reflection Radiometer (ASTER) GDEM v2 DEM that was used has a resolution of 15 m. The DEM was resampled by the Cubic convolution method to a resolution of 2m to have equal resolutions of the land use map and DEM.

3.3.3 Management practices

3.3.3.1 Irrigation

The abstraction of water due to irrigation was quantified using discharge measurements. Two discharge measurement locations of the Wosha river were chosen; one upstream (lat 7, 05 28; lon 38, 37 40) and one downstream (lat 7, 04 31; lon 38, 35 20) (Appendix: 8.2 Location flow velocity measurement points). The upstream location of the Wosha stream was assumed not to be affected by irrigation. But, irrigation took place in the downstream part. This means that the difference in stream flow between both locations could be explained by irrigation abstraction.

In order to model the irrigation correctly, more than 20 short interviews with local farmers about the crop cycle, timing of irrigation, amount of irrigated water, regulations of irrigation and irrigated water source were done. Those interviews provided some information about irrigation management. For example that no irrigation takes place during the *kiremt*.

3.4 Modelling stages

The hydrologic model was finalized after performing four stages (Fig 7). The first stage was creating a model of the Wosha upstream catchment. This area is assumed not to be affected by irrigation and the swamp. Furthermore it was assumed that the hydrological characteristics of this area, which is at high elevation (plateau), are different than the characteristics of the area downstream. The Wosha upstream catchment has been chosen among the six other streams since a long discharge record was available. The Wosha subbasin model was then calibrated and validated. The calibrated parameters were extended to the other subbasins at the plateau.

The observed stream flow drop due to irrigation was modeled in the second stage by applying auto-irrigation to the crops: khat, sugarcane, maize and green beans. The auto-irrigation is triggered when the actual plant water stress falls below the 0.95 threshold. The chosen subbasins for irrigation are shown in figure 7.

In the third stage, 23 reservoirs were applied to the subbasins in the swamp area. Subsequently, these reservoirs were calibrated and validated. SWAT doesn't allow to model one reservoir since the reservoir surface area is bound to a maximum area.

Finally, all remaining uncalibrated subbasins were calibrated and validated. This fourth and final stage is named as the Awassa calibration.

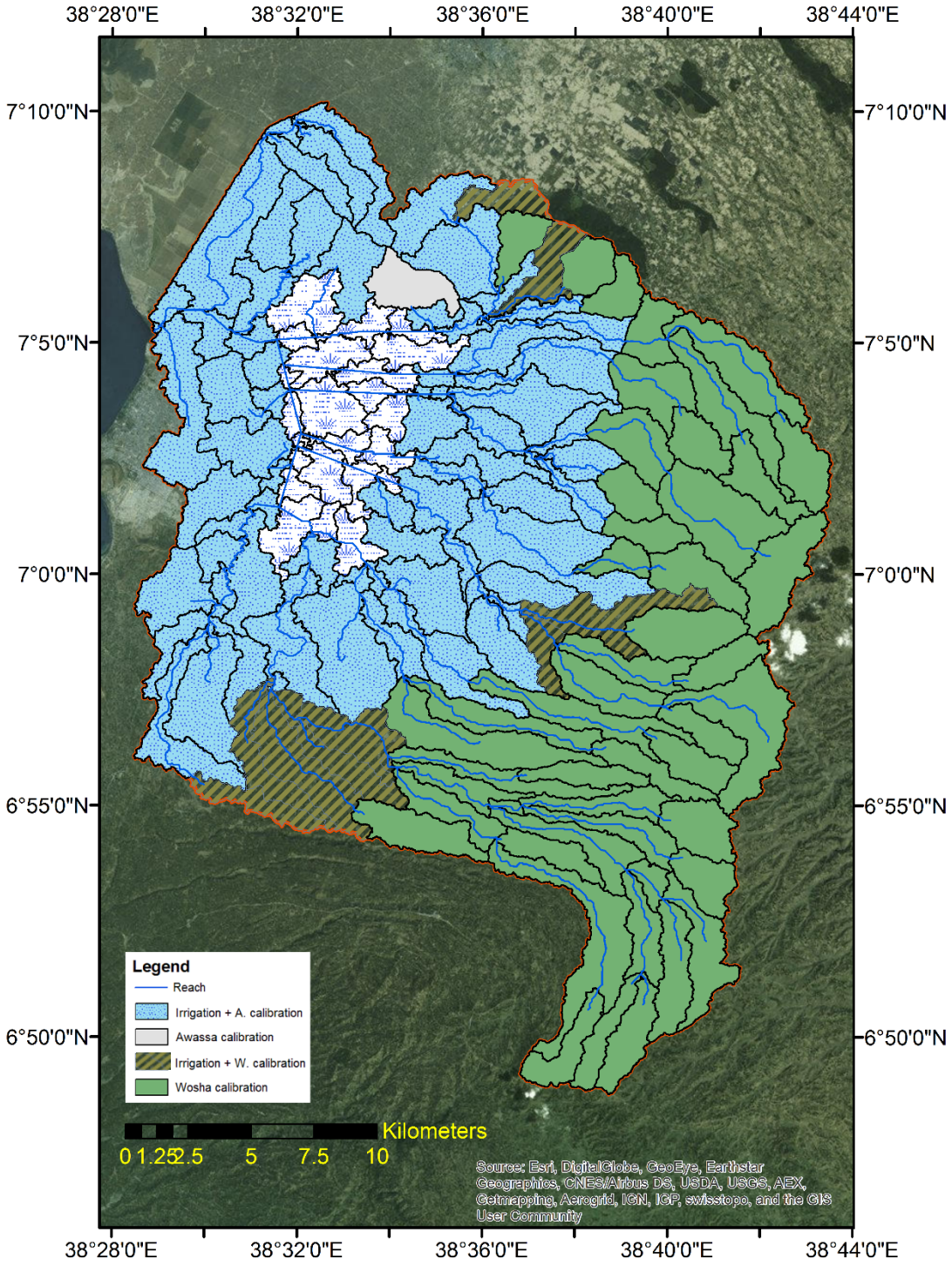

Figure 7: Four model stages that were applied: firstly calibrating + validating the Wosha subbasin (plateau), secondly implementing irrigation, thirdly adding and calibrating + validating the 23 reservoirs and at last calibrating the remaining subbasins named the Awassa calibration stage (A. = Awassa; W. = Wosha).

3.5 Calibration and validation

Calibration and validation of the three stages: Wosha subbasin, reservoir stage and Awassa calibration were performed by the program SWAT-CUP (v5.1.6.2). This auto-calibration program provides several methods to calibrate a SWAT model. The method that was chosen is SUFI-2. SUFI-2 performs numerous iterations which can be chosen manually. The parameters

Each simulation ran by between 250 and 500 iterations resulted into a higher certainty and a smaller parameter range. Choosing these parameters is an important step. Parameterization was a procedure before calibration starts to identify the most sensitive parameters. Furthermore, it was necessary to adjust the parameter range in a natural way instead of choosing some random forced numbers provided by the program. It was needed to select specified subbasins before calibration of the three different stages. Otherwise the parameters would be calibrated double. At last, some parameters needed to be adjust by a percentage instead of an absolute number to remain spatial diversity on HRU scale.

The observed data for calibration and validation was not used in chronologic order. The observed data has been changed to an order based on annual mean intensities. This method reduces effects created by a trend in the observed discharge series.

The Coefficient of determination (R^2), the Nash-Sutcliffe efficiency (NSE), and the percent bias (PBIAS) were used to statistically review the calibration and validation results.

The Coefficient of determination (R^2) is calculated by:

$$R^2 = \frac{\left[\sum_i (Q_{m,i} - \overline{Q}_m)(Q_{s,i} - \overline{Q}_s)\right]^2}{\sum_i (Q_{m,i} - \overline{Q}_m)^2 \sum_i (Q_{s,i} - \overline{Q}_s)^2} \quad [20]$$

where Q is the discharge variable, and m and s stand for measured and simulated, i is the i^{th} measured or simulated data. The R^2 values range from 0 to 1.0. The higher the value the less error variance between the observed and simulated discharge variable.

Nash-Sutcliffe efficiency (NSE) is calculated by (Nash and Sutcliffe, 1970):

$$NSE = 1 - \frac{\sum_i (Q_m - Q_s)_i^2}{\sum_i (Q_{m,i} - \overline{Q}_m)^2} \quad [21]$$

The NSE values can range from $-\infty$ to 1.0 where 1.0 is the optimal value.

Percent bias (PBIAS) is calculated by (Gupta, 1999):

$$PBIAS = 100 \cdot \frac{\sum_{i=1}^{n} (Q_m - Q_s)_i}{\sum_{i=1}^{n} Q_{m,i}} \quad [22]$$

PBIAS measures the average tendency of the simulated values to be larger or smaller than their observed ones (Gupta, 1999). The PBIAS values range from -10 to 10 with the optimal value of 0.0. Accurate model simulation can be indicated by low PBIAS magnitude values. Positive PBIAS values represents model underestimation bias, whereas model overestimation bias is indicated by negative PBIAS values.

3.6 Statistics

The precipitation and precipitation trends have been analyzed with a linear regression fit. The linear regression fit is as follows:

$$Y = a + b \cdot t \quad [23]$$

where Y stands for precipitation [mm], a (y-axis intercept) and b (slope of the trend) are the linear regression coefficients. These coefficients have been obtained by using the least square method.

The independent two sampled t-test has been used to determine the significance of the irrigation withdrawals and the effects of the swamp. The t-test is calculated as:

$$t = \frac{\bar{x}_1 - \bar{x}_2}{\sqrt{s^2\left(\frac{1}{n_1} + \frac{1}{n_2}\right)}} \quad [24]$$

where $\bar{x}_1$ and $\bar{x}_2$ are the sample means, s^2 is the pooled sample variance, n_1 and n_2 are the sample sizes and t is a Student t quantile with $n_1 + n_2 - 2$ degrees of freedom. To calculate the sample variance the following equation has been used.

$$s^2 = \frac{\sum_{i=1}^{n_1}(x_i - \bar{x}_1)^2 + \sum_{j=1}^{n_2}(x_j - \bar{x}_2)^2}{n_1 + n_2 - 2} \quad [25]$$

4. Results

4.1 Measured hydrological data

4.1.1 Precipitation

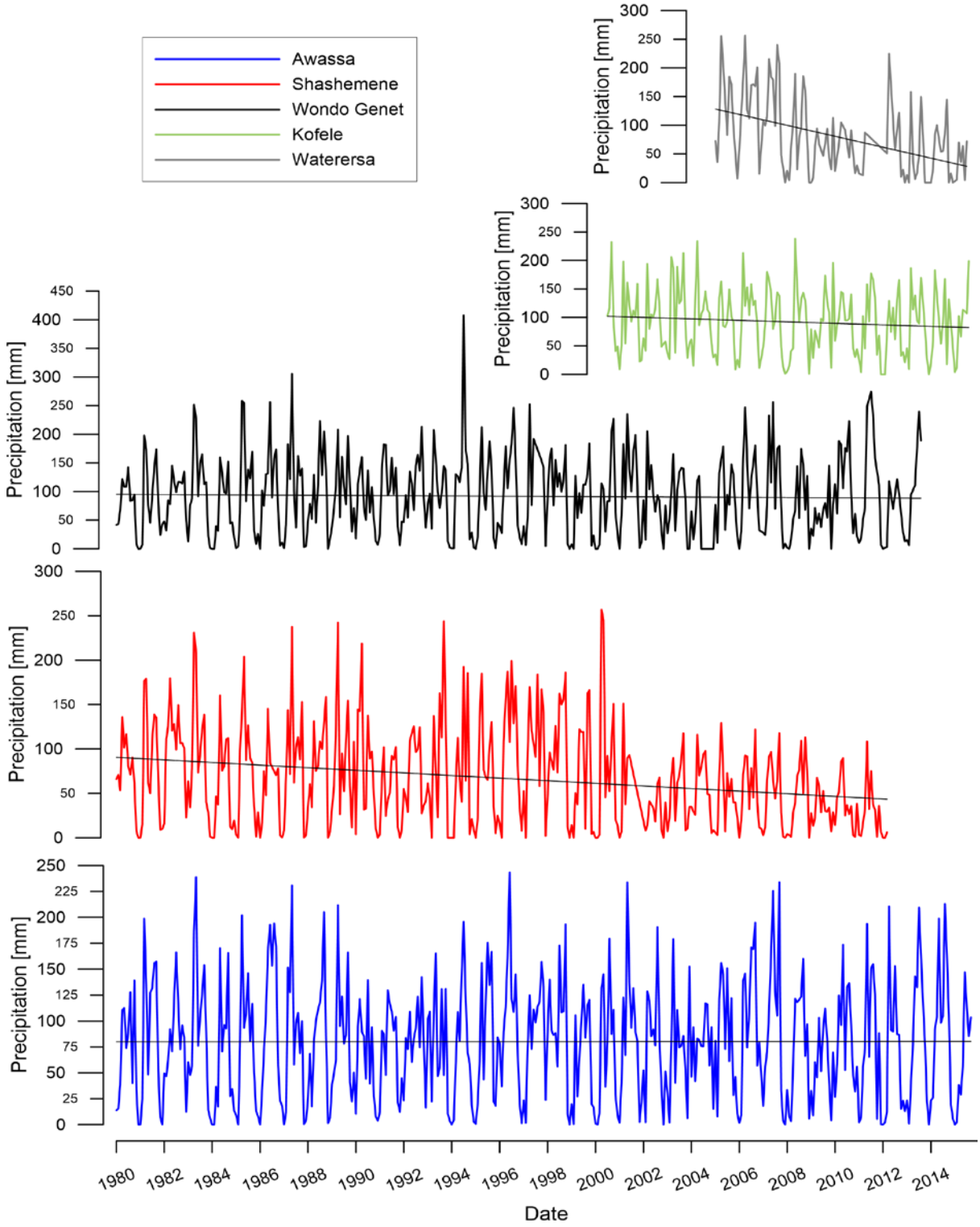

Figure 8: Precipitation time series (monthly scale) measured by five different rain gauges; respectively Awassa (years 1980-2015), Shashemene (years 1970-2012), Wondo Genet (years 1980-2013), Kofele (years 2000-2015) and Waterersa (years 2005-2015). Every time series is fitted with a linear regression line; Awassa (y = 0.0009x + 79.917), Shashemene (y = -0.1222x + 90.756, sig., p<0.05), Wondo Genet (y = -0.0167x + 95.0.), Kofele (y = -0.1091x + 102.02) and Waterersa (y = -0.7940x + 129.21; sig., p<0.05)

The precipitation time series measured by the five rain gauges are plotted in figure 8. The Awassa and the Wondo Genet time series show no trend. But, slightly decreasing precipitation trends are observed in the Shashemene, Kofele and Waterersa time series. The decreasing trend is gentle but noticeable. The Waterersa (sig., $p<0.05$[1]) precipitation trend is steeper than the Shashemene (sig., $p<0.05$) and Kofele (not sig.) trends. The Shashemene precipitation trend results in a decrease of 16.1 mm every decade, whereas the Waterersa trend results in a decrease of 95.2 mm and the Kofele trend results in a decrease of 13.1 mm. The decreasing trends of Kofele and Waterersa do not provide long term information since the Waterersa and Kofele time series are too short to show any long-term trends. A minimum of about 30 years is required to show any long-term trend. It is remarkable that decreasing trends are only observed at high elevation: on the plateau (Kofele and Waterersa) and in the North (Shashemene).

4.1.2 Streamflow

The discharge time series of the Wosha stream and Tikur Woha are plotted in figure 9. The seasonal fluctuations are clearly visible in both discharge time series. The annual minimum monthly Tikur Woha discharge is about 1.1 m^3/s during most dry seasons and the absolute monthly minimum was 0.3 m^3/s in January 1981. The annual maximum monthly discharge is around 4.4 m^3/s during most wet seasons and the absolute monthly maximum was 5.1 m^3/s in October 1992. The long term trend shows a statistically significant increase in discharge of approximately 1.7 m^3/s over the period 1981-2007 ($p<0.05$). The increase in discharge is found to be 0.064 m^3/s annually. The annual minimum monthly Wosha discharge is about 0.33 m^3/s during most dry seasons and the absolute monthly minimum was 0.21 m^3/s in January 1981. The annual maximum monthly discharge is around 1.0 m^3/s during most wet seasons and the absolute monthly maximum was a discharge peak of 2.1 m^3/s in October 1983. The long term trend shows a statistically significant increase in discharge of approximately 0.35 m^3/s over the period 1980-1996 ($p<0.05$). The increase in discharge is found to be 0.023 m^3/s annually. The increase in discharge of the Tikur Woha River is almost three times more than the increase in the Wosha discharge.

[1] Statistical significance level using the 95% confidence interval ($p<0.05$).

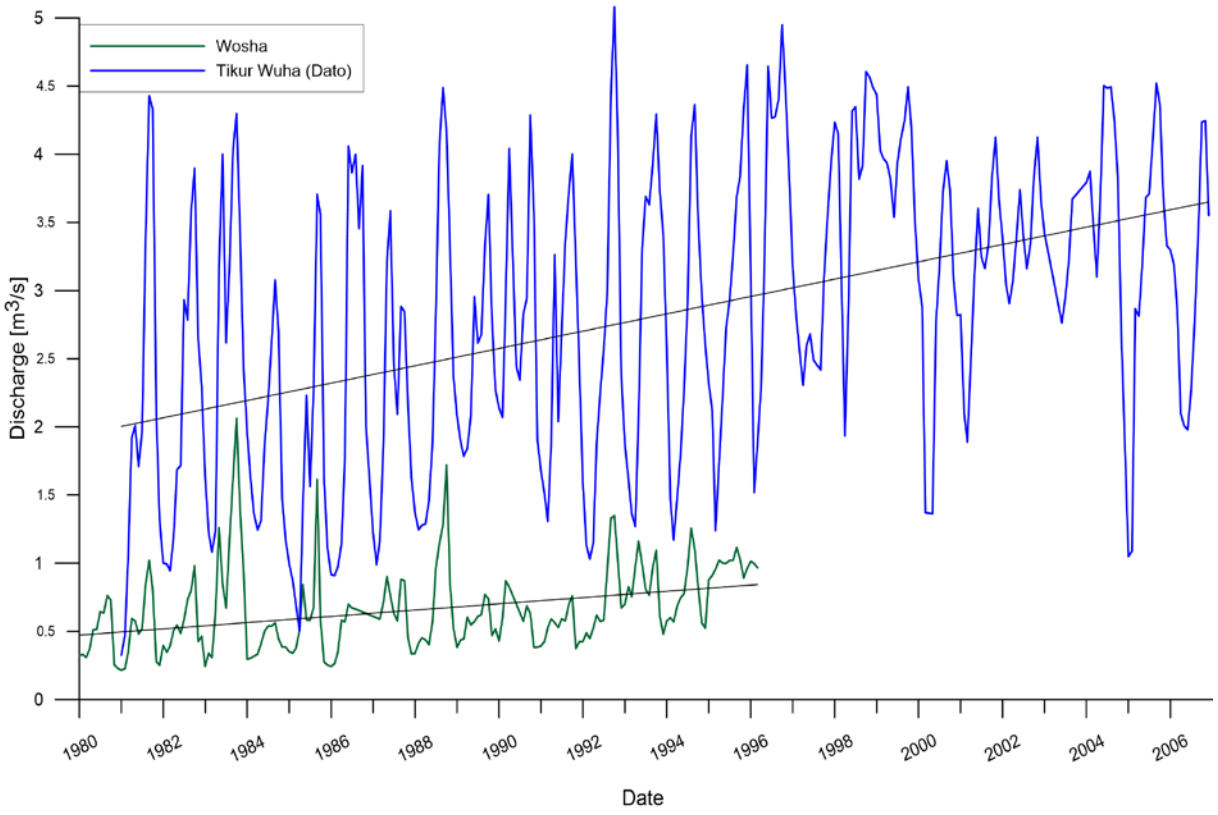

Figure 9: Wosha (years 1980-1996) and Tikur Woha (years 1981-2006) discharge time series (monthly scale). Every time series is fitted with a linear regression line; Tikur Woha (y = 0.0053x + 1.998, sig.) and Wosha (y = 0.0019x + 0.471, sig.).

The discharge measured by the Aqua Data SENSA RC2 Water Velocity Meter during fieldwork is displayed in figure 10. The plot contains discharge data points from the localities Wosha upstream, Wosha downstream, Worka, Abosa, Wedesa, Hallo, Shonkora and Boga / Galchacha (Appendix 8.2: Location flow velocity measurement points). The stream velocity is measured during the transition from *Kiremt* to *Bega*. At the end of K*iremt* the Wosha stream has the highest discharge of all other streams. During B*ega* the Wedesa has the highest discharge.

A decrease in discharge can be seen clearly during the transition from the wet to the dry season. Two different trends can be distinguished. The streams Wosha US, Wedesa, Boga/Galchacha and Abosa have a decreasing trend at a relative equal rate. But the decreasing trend of the streams Wosha DS and Worka is much steeper. In November the discharge at both locations reaches zero m^3/s due to diversion of both stream channels. The diverted water is being used for irrigation purposes. The measurement locations of the streams of both trends are different. The locations of the Wosha DS and the Worka are further downstream and closer to the swamp than the locations of the streams Wosha US, Wedesa, Boga/Galchacha and Abosa. The measurement locations of these streams are more upstream and closer to the rim in the east; especially the location of Wosha US. The streamflow further downstream is affected more by irrigation withdrawals, which explains the steeper discharge decrease rate for the streams Wosha DS and Worka.

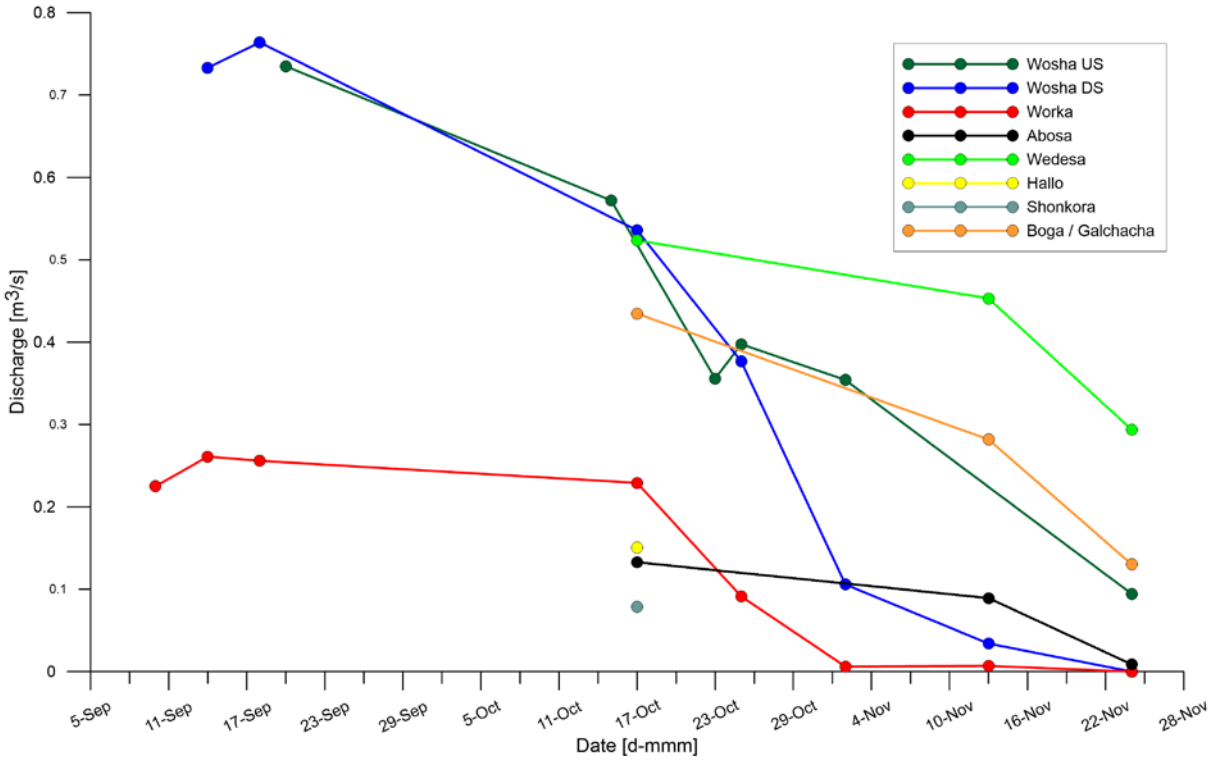

Figure 10: Discharge data points from the streams Wosha US (upstream), Wosha DS (downstream), Worka, Abosa, Wedesa, Hallo, Shonkora and Boga / Galchacha measured during the transition from the Kiremt to the Bega.

4.1.3 Awassa lake level

The water level of Lake Awassa fluctuates over time. In figure 11 the fluctuations in lake level are shown. The lake level was in October 1969 at 1679.5 meter above mean sea level (m.a.m.s.l.). The fluctuation annually due to seasonality is between 0.5 and 1.0 meter. The highest lake level was in October 1998. The measured lake level was 1682.3 m.a.m.s.l. This level caused flooding near Lake Awassa.

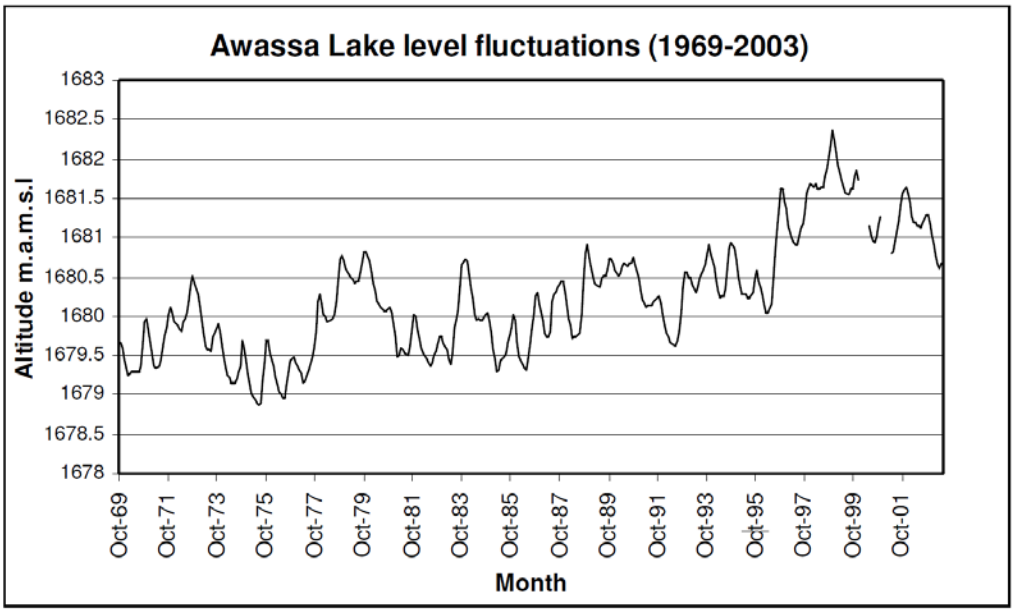

Figure 11: Awassa lake level fluctuations (1969-2003) (Gebreegziabher, 2004)

An increasing trend in the lake level of Awassa has been showed by Belete et al. (2015), Alemayehu Abiye (2008), Ayenew and Gebreegziabher (2006) and Gebreegziabher (2004). The increase of the lake level and its monotonic trends is showed in more detail in figure 12.

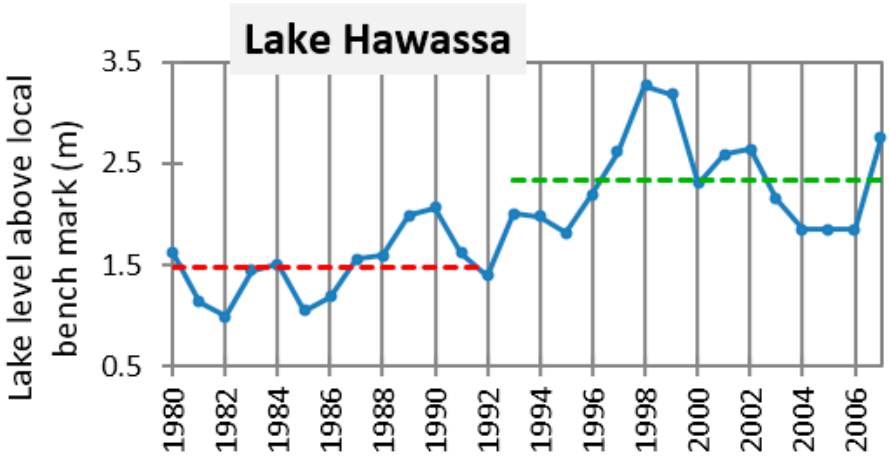

Figure 12 Awassa lake level fluctuations (1980-2006)

4.2 Model performance

4.2.1 Parameterization

In figure 7 four model stages that were applied are displayed. These four stages were in chronologic order: the calibration of the Wosha subbasin model, implementing irrigation, adding and calibrating the reservoirs and calibration of remaining subbasins (Awassa calibration). The five or six most sensitive parameters of each stage except for irrigation were calibrated and validated. The most sensitive parameters were obtained by reviewing literature (J. G. Arnold et al., 2012; Abbaspour et al., 2015b; Abbaspour et al., 2015a). The six parameters that were calibrated during the first stage are curve number for the moisture condition II, available water capacity, soil evaporation compensation factor, groundwater delay, the threshold depth of water in the shallow aquifer required for return flow to occur and baseflow alpha factor (Appendix: 8.7 SWAT model (Table 3)). The five most sensitive reservoir parameters are listed in (Appendix: 8.7 SWAT model (Table 4)). These five parameters are the hydraulic conductivity of the reservoir bottom, minimum and maximum daily outflow for the month, the Lake evaporation coefficient and the average daily principal spillway release rate. The parameters of the remaining uncalibrated areas have been calibrated during the fourth stage. The five most sensitive of these parameters are listed in (Appendix: 8.7 SWAT model (Table 5)). Curve number for the moisture condition II, available water capacity, the threshold depth of water in the shallow aquifer required for return flow to occur, the groundwater "revap" coefficient and the threshold depth of water in the shallow aquifer for "revap" to occur are the parameters used for calibration.

4.2.2 Calibration and validation

The statistical results of calibrating and validating the Wosha subbasin, the reservoirs and the Awassa model stages are listed in table 6,7 and 8 respectively (Appendix: 8.7 SWAT model. The calibration of the Wosha subbasin, and thus the plateau region (Fig. 7), is based on the Wosha discharge series from 1987 to 1992. The mean observed flow during this time series is 0.73 m^3/s whereas the mean simulated flow is 0.72 m^3/s for the same period. They show a very close similarity. The mean observed flow during the validation time series, ranging from 1993 to 1996, is 0.72 m^3/s whereas the mean simulated flow

is 0.70 m^3/s. The Coefficient of Determination (R^2) for calibration and validation is respectively 0.29 and 0.05. This indicates a high error variance in the model. The Nash and Sutcliffe Efficiency (NSE) during the calibration period is 0.29 which is viewed as within acceptable levels of performance. The NSE value of 0.0 during the validation period indicates a simulation consisting of the mean of the observations. The simulation results shows a percent bias (PBIAS) of 0.7 and 3.5 for calibration and validation respectively. Both PBIAS values indicate model underestimation. Furthermore the calibration PBIAS indicates a more accurate model simulation compared to the validation PBIAS.

The calibration of the 23 reservoirs is based on the Tikur Woha discharge series from 1987 to 2001. The period ranging from 2002 to 2006 is used for validation of the five reservoir parameters. During the calibration period the mean observed Tikur Woha flow is 2.91 m^3/s whereas the mean simulated flow is 2.95 m^3/s. The mean observed Tikur Woha flow during the validation period is 3.31 m^3/s whereas the mean simulated flow is 2.96 m^3/s. The R^2 value for calibration and validation is respectively 0.24 and 0.01. The NSE value stands 0.22 and -0.18 for calibration and validation respectively. According to the PBIAS value of -1.4 for calibration period the model slightly overestimates stream flow during this period. For the validation period however, the PBIAS value of 10.5 indicates model underestimation. The model simulation during the calibration period is more accurate than the simulation during the validation period.

Calibration and validation of remaining subbasins, called the Awassa calibration is the final modelling stage. These results indicate therefore the performance of the hydrological SWAT model. The calibration and validation is based on the Tikur Woha discharge series. The calibration period ranges from 1987 to 2001 and the validation period ranges from 2002 to 2006. The mean observed flow during the calibration period is 2.91 m^3/s whereas the mean simulated flow is 2.94 m^3/s for the same period. The mean observed flow during the validation time series is 3.31 m^3/s whereas the mean simulated flow is 3.25 m^3/s. The R^2 value for calibration and validation is respectively 0.28 and 0.01. The NSE is 0.25 for the calibration period and -0.43 for validation period. According to NSE method, the model results for validation are not acceptable. The PBIAS value of -1.2 for calibration period indicates that the model slightly overestimates stream flow during this period. For the validation period however, the PBIAS value of 1.9 indicates model underestimation. The PBIAS value reveals that the model simulation during the calibration period is slightly more accurate than the simulation during the validation period.

The discharge of the Tikur Woha at Dato location (Appendix 8.2 Location flow velocity measurement points) simulated by the hydrological SWAT model is presented in figure 13. The simulated discharge time series covers the period from 1987 to 2015. The annual average discharge simulated by the model is 2.59 ± 0.25 m^3/s. The amplitude of the simulated peak and baseflow is in most periods lower than the observed Tikur Woha discharge series. Especially in the period 2000 to 2006. In the years 1988 and 1995 to 1998 the overlap between the simulated and observed peak and baseflow is high. The timing of the peak flows are simulated satisfactory.

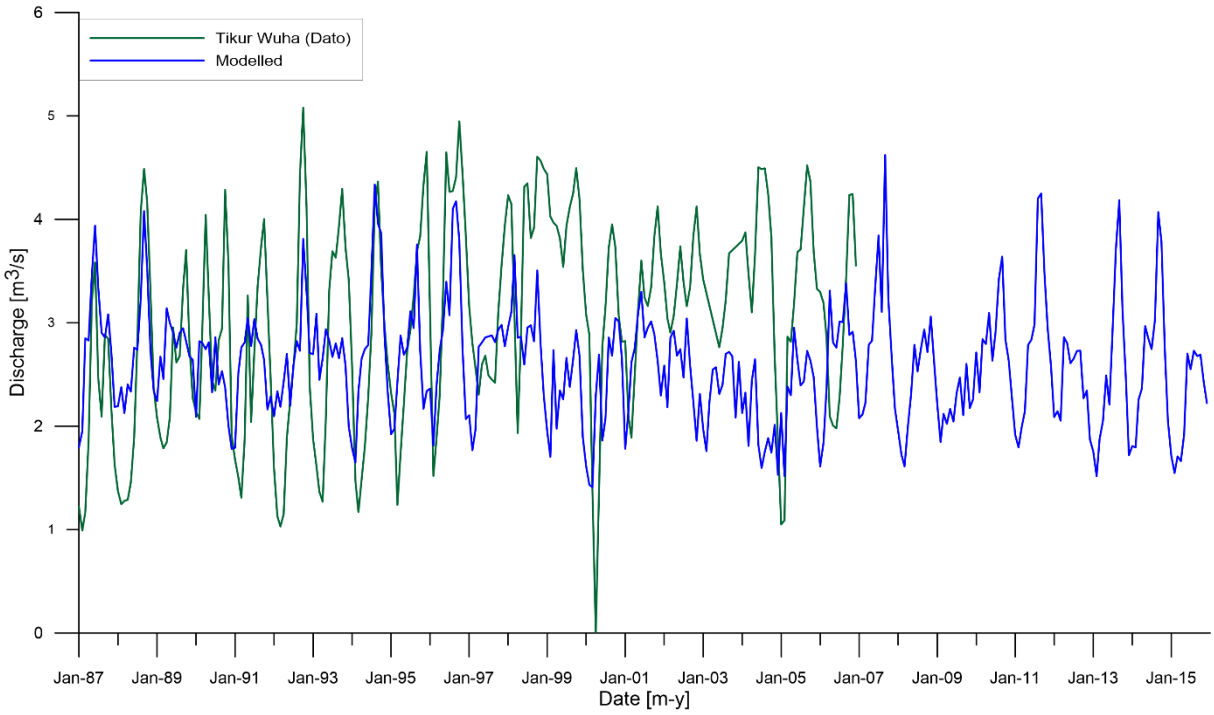

Figure 13: Simulated Tikur Woha discharge (blue) versus observed Tikur Woha discharge (green).

4.3 Model results

4.3.1 Irrigation

4.3.1.1 Wosha subbasin

In figure 14 the Wosha discharge series of two simulation runs are plotted. One of these two runs is a model run simulated under normal conditions. The second simulation run is a scenario run performed without irrigation in the Wosha subbasin. The dry months, December to March (*Bega* period), are highlighted in figure 14 to emphasize the main irrigation period. The auto-irrigation performed by SWAT irrigates almost fully within this period. In 2004 SWAT irrigates crops even during the wet months. This could be explained by the lack of precipitation in those months which causes water stress and therefore SWAT triggers irrigation. In the years 1990, 1998 and 2010 the irrigation has only a minor effect on the Wosha discharge. A high Wosha discharge level could indicate a wetter than normal dry season and therefore the water stress threshold was not exceeded often. The auto-irrigation method simulates the decrease in discharge overall very well. The mean monthly discharge simulated by the run with irrigation is 0.49 ± 0.25 m^3/s. The mean monthly simulated without irrigation is 0.52 ± 0.22 m^3/s. The difference in percentage between both monthly means is plotted in figure 15. The decrease in discharge starts in the month November (-6.1 ± 11%) and lasts till April (-5.3 ± 10%). The decrease in discharge is significant for the months December*, January* and February* [2]. The difference in monthly discharge between both runs is at maximum in February. The Wosha discharge drops due to irrigation by -31.3 ± 18.6% (sig.*, p<0.01). The discharge difference in the month January becomes secondly with a decrease of -26.0 ± 14.4% (sig.*, p<0.01).

[2] Two sample t-test (one-tailed). * Statistical significance level using the 99% confidence interval (p<0.01).

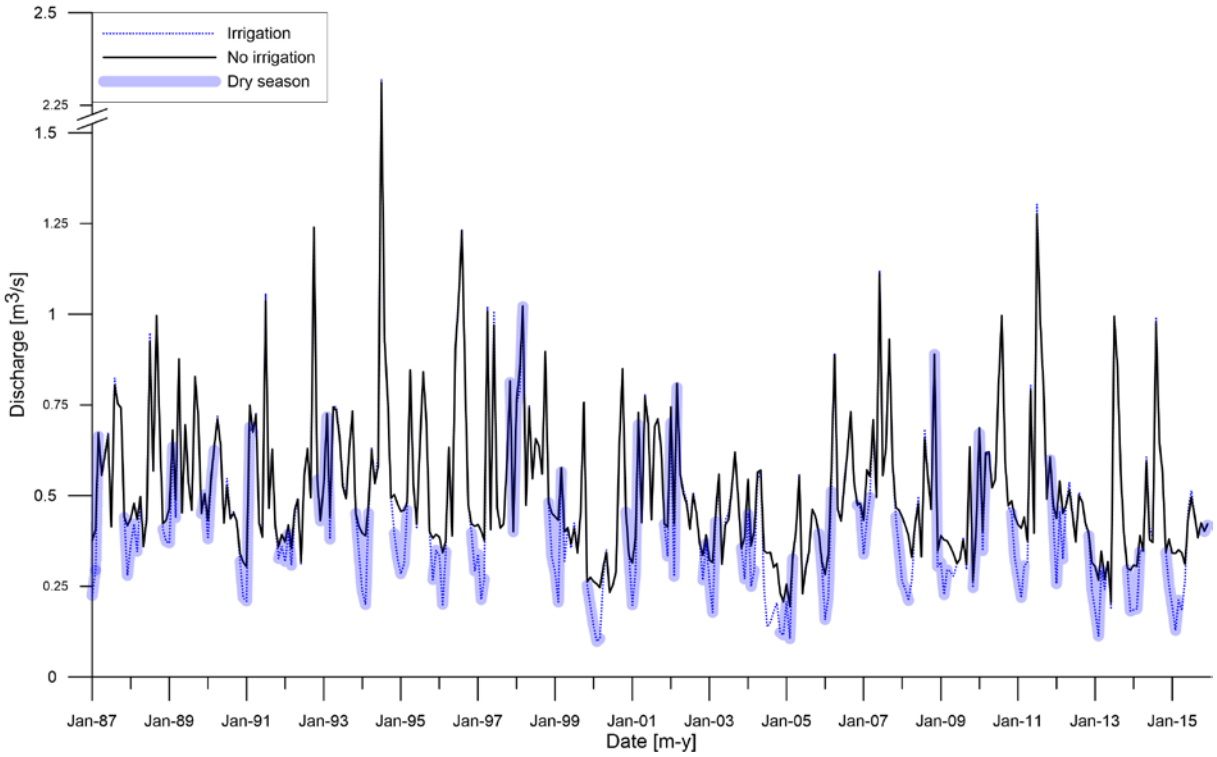

Figure 14: Wosha discharge series of two simulation runs: one run is a normal calibrated simulation run with irrigation and the swamp, and the other is a scenario run without irrigation in the whole subbasin. Dry months (December to March) are highlighted.

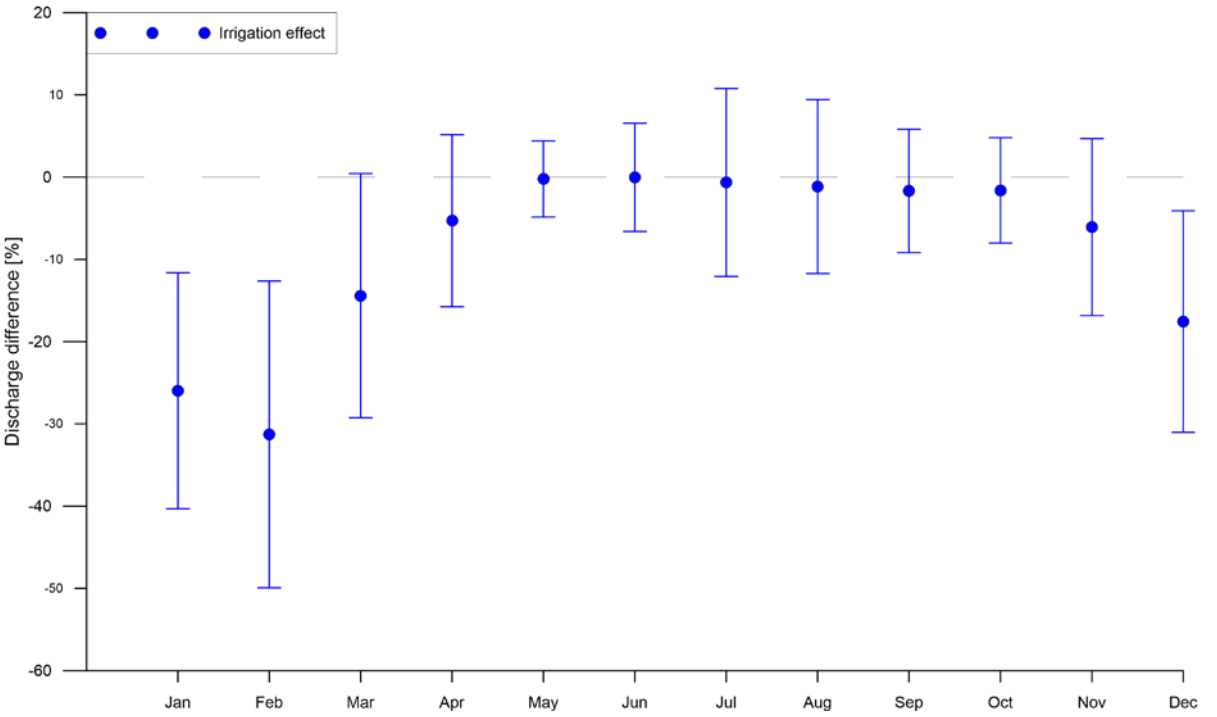

Figure 15: The mean monthly percentage difference between a normal calibrated simulation run with irrigation and is a scenario run without irrigation in the whole subbasin. The decrease in discharge is significant for the months December, January* and February*. A two sample t-test (one-tailed) has been used to test the statistical significance of the decreasing trend between the discharge means.* Statistical significance level using the 99% confidence interval ($p<0.01$). The plotted error bars represents the standard deviation.*

4.3.1.2 Tikur Woha subbasin

In figure 16 the Tikur Woha discharge series of two simulation runs are plotted. One run is a normal calibrated simulation run with irrigation and the swamp. The other is a scenario run without irrigation in the whole subbasin. The difference in percentage between both monthly means is plotted in figure 17. The mean monthly discharge simulated by the run with irrigation is 2.71 ± 0.65 m^3/s. The mean monthly simulated without irrigation is 2.77 ± 0.55 m^3/s. Clearly visible is the decrease in discharge due to irrigation in the dry months (December to March). These dry months are highlighted in figure 16. The decrease in discharge is significant for the months December*, January* and February** [3]. Almost all discharge drops are highlighted except for the drop in the rain season in 2004. The monthly discharge difference between both runs is at maximum in February. In this month the average decrease is 14 ± 7.7% ** due to irrigation in the subbasin. The decrease in discharge starts in the month December (-5.8 ± 4.2%*) and lasts till March (-6.7 ± 7.6%). Remarkable is the increase of discharge simulated by the scenario run without irrigation in the months May, June and July. The increase in discharge is for all months 2.2% and a standard deviation between 3.3 and 4.7%.

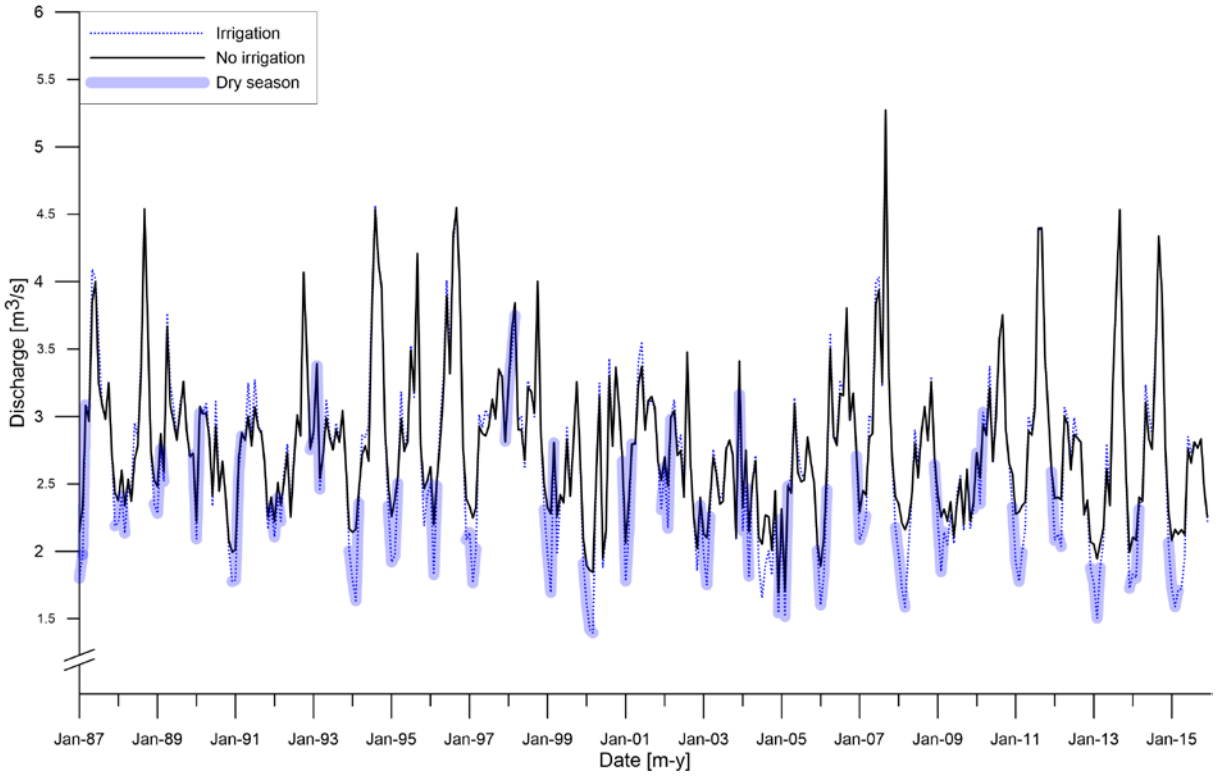

Figure 16: Tikur Woha discharge series of two simulation runs: one run is a normal calibrated simulation run with irrigation and the swamp, and the other is a scenario run without irrigation in the whole subbasin. Dry months (December to March) are highlighted.

[3] Two sample t-test (one-tailed). * Statistical significance level using the 99% confidence interval (p<0.01). ** Statistical significance level using the 90% confidence interval (p<0.1).

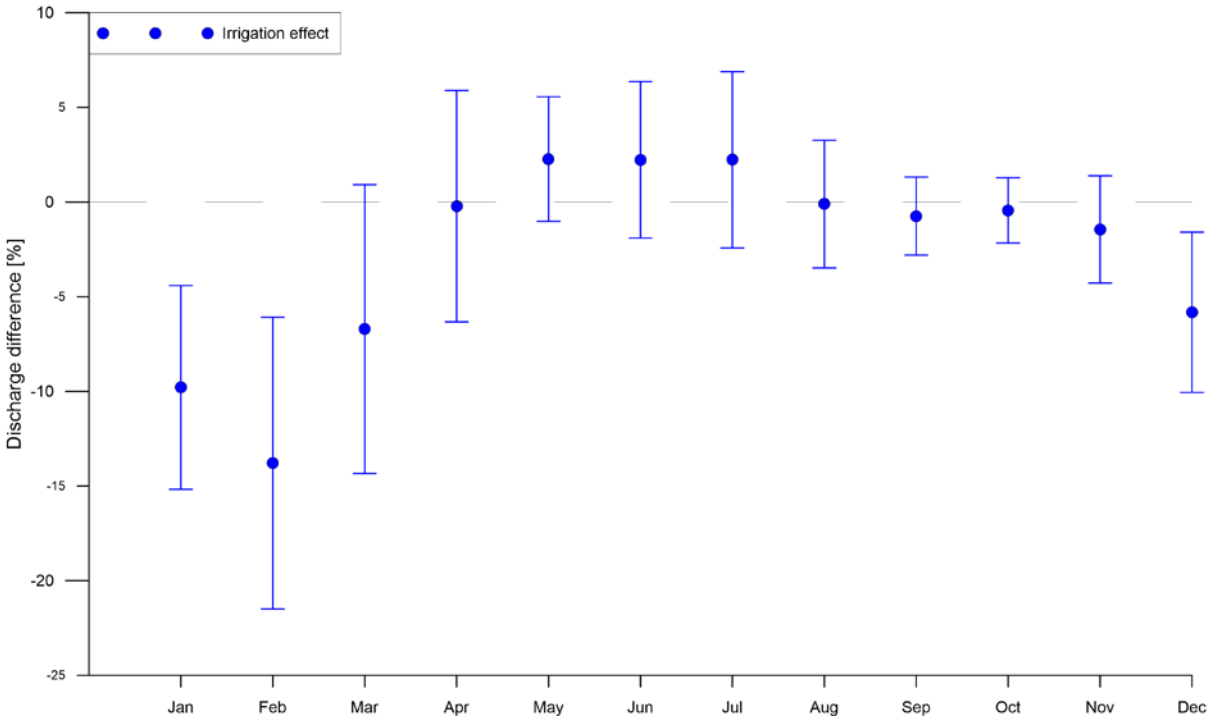

Figure 17: The mean monthly percentage difference between a normal calibrated simulation run with irrigation and is a scenario run without irrigation in the whole subbasin. The decrease in discharge is significant for the months December, January* and February**. A two sample t-test (one-tailed) has been used to test the statistical significance of the decreasing trend between the discharge means.* Statistical significance level using the 99% confidence interval (p<0.01). ** Statistical significance level using the 90% confidence interval (p<0.1). The plotted error bars represents the standard deviation.*

4.3.2 Swamp

The simulated Tikur Woha discharge at the outlet of the catchment, thus into Lake Awassa, versus a discharge scenario without the swamp is plotted in figure 18. In this scenario the area of the swamp has been replaced by agricultural fields (sugarcane). Those agricultural fields are irrigated by the same rate as modelled for the crops in surrounding areas. The monthly mean simulated Tikur Woha discharge, with the swamp taken into account, is 2.71 ± 0.65 m^3/s. The monthly mean simulated Tikur Woha discharge, with irrigated sugarcane fields, is 5.68 ± 4.54 m^3/s (Fig. 18). The same simulated discharge series but without irrigation results into a mean monthly discharge of 5.95 ± 4.25 m^3/s. The magnitude of discharge intensities from the no reservoirs simulation is enormously increased compared to the simulation with reservoirs. Every peak flow in the time series has been increased in magnitude. Common peak flows, between a discharge range of around 3.0 to 4.5 m^3/s, increased to peak flows between 9.0 to 15 m^3/s. The baseflow during the dry months remains mostly at the same discharge level as the simulation with reservoirs. However during the years 2005 to 2007 and 2011 to 2012 the baseflow doubles.

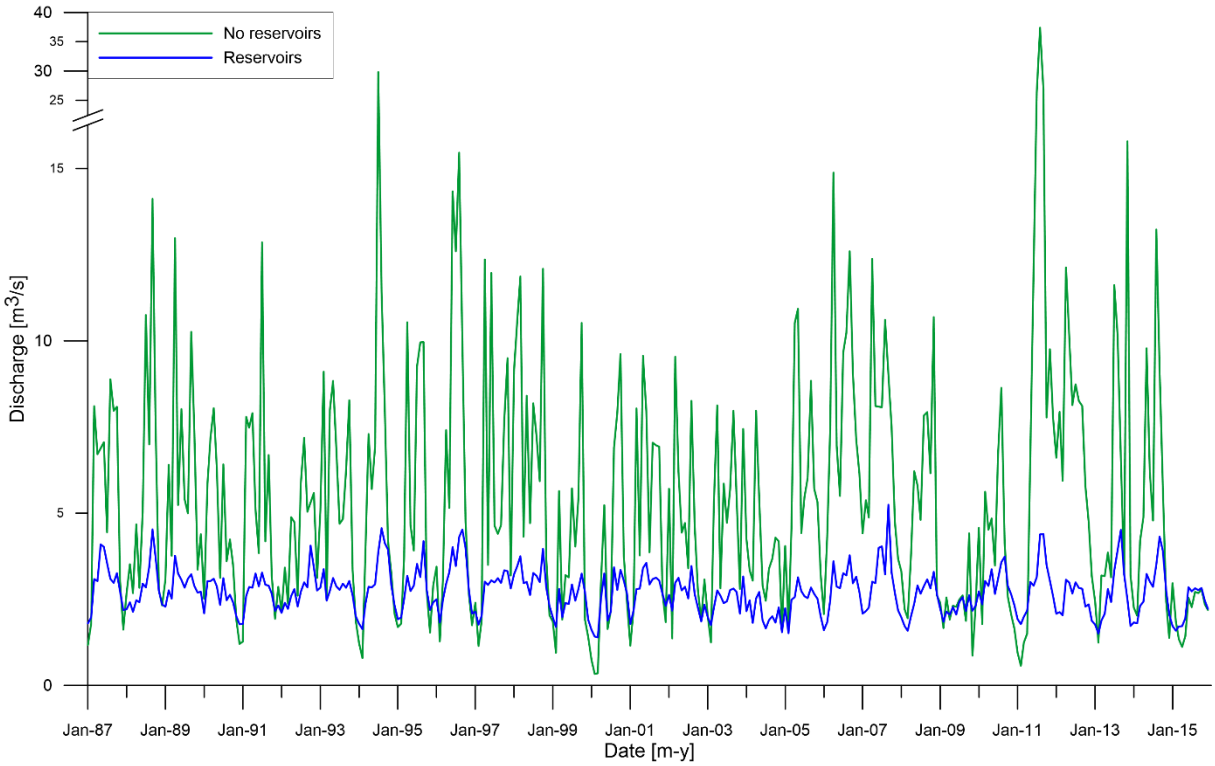

Figure 18: Simulated Tikur Woha discharge series of both a normal simulation run and scenario run without the swamp. The area of the swamp has been replaced by irrigated sugarcane fields.

Monthly discharge differences in percentages between a normal simulation run and two scenario runs without the swamp is plotted in figure 19. The discharge during the wet months increases with values between 100 and 150% in both runs. The maximum monthly discharge increase is 152% in July for the non-irrigated run and an increase of 177% in July for the irrigated run. The minimum monthly discharge increase is 23% in December for the non-irrigated run and an increase of 57% in July for the irrigated run. All increased discharges between both simulation under normal condition with reservoirs and the non-irrigated without reservoirs are statistical significant using the 99% confidence interval ($p<0.01$)[4].

The increased discharges between the simulations under normal condition with reservoirs and the simulation with irrigated sugarcane fields (without reservoirs) are statistical significant as well[5]. However the significance level in the months December to February is lower since it makes use the 95% confidence interval ($p<0.05$*). The significance level in all other months is high ($p<0.01$**). The error bars represents the standard deviation. The standard deviation is accordingly to both scenario runs the highest in July.

[4] Two sample t-test (one-tailed). Statistical significance level using the 99% confidence interval ($p<0.01$).
[5] Two sample t-test (one-tailed). * Statistical significance level using the 99% confidence interval ($p<0.01$).
** Statistical significance level using the 95% confidence interval ($p<0.05$).

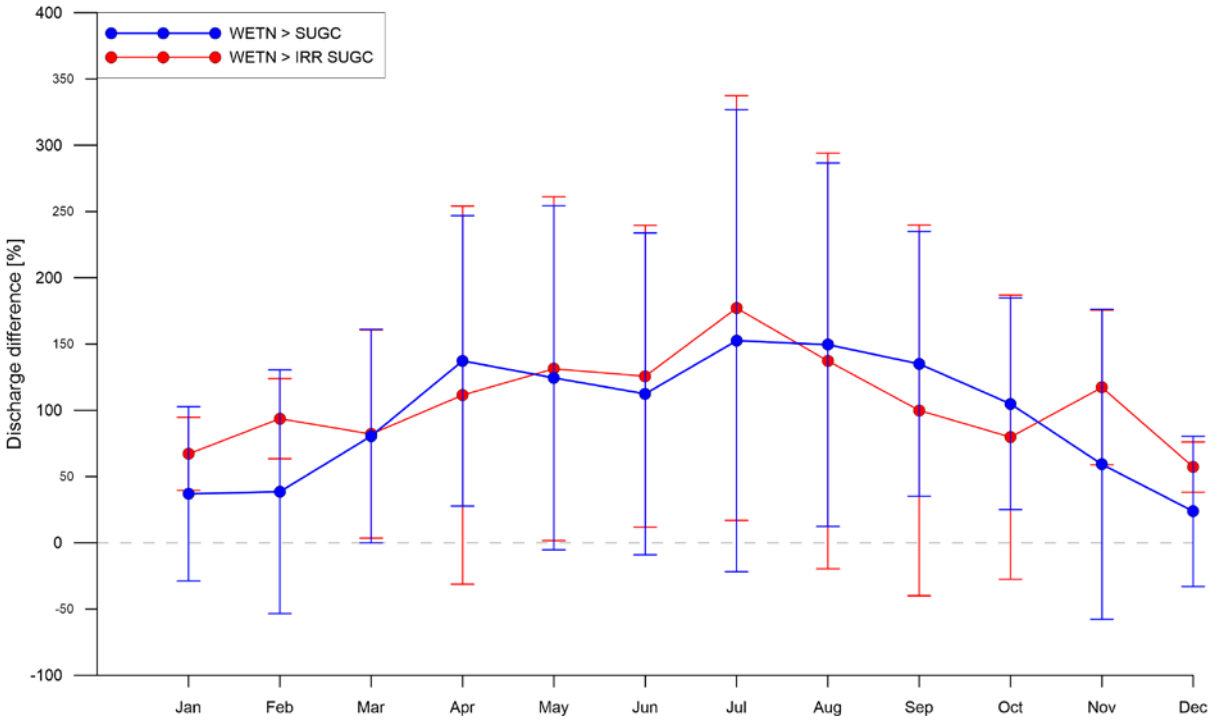

Figure 19: Monthly discharge difference in percentage between normal simulation run and two scenario runs without the swamp. The blue coloured graph is a scenario run with sugarcane fields instead of a swamp and the red coloured graph is a scenario run with irrigated sugarcane fields. The plotted error bars represents the standard deviation.

5. Discussion

5.1 Hydrology

Precipitation is important for the water balance. Precipitation changes can influence the water balance in the Awassa catchment. The Awassa and the Wondo Genet time series show no trend for the years 1980-2014. No trends for the Awassa time series ware showed earlier by Herder (2013). But, slightly decreasing precipitation trends are observed in the Shashemene, Kofele and Waterersa time series. However, a minimum of about 30 years is required to show any long-term trend. The Waterersa and Kofele precipitation time series range from 2006 to 2015 and from 2001 to 2015, respectively. These time series are too short to provide long-term information. Therefore the precipitation in the Awassa catchment shows no long-term trend. Periodic events, such as ENSO phenomena, do not show clear effects on the precipitation in the Awassa catchment.

Both streamflow of the Wosha and Tikur Woha river significantly increased during the observed period from 1980 to 1996 and 1981 to 2006, respectively ($p<0.05$). This is in line with previous studies (Gebreegziabher, 2004; Belete, 2013; Herder, 2013). The long-term Tikur Woha trend shows a statistically significant increase in discharge of approximately 1.7 m^3/s over the period 1981-2007 ($p<0.05$). The long-term Wosha trend shows a statistically significant increase in discharge of approximately 0.35 m^3/s over the period 1980-1996 ($p<0.05$). The long-term significant increasing trend of discharge cannot be explained by precipitation changes, since the Awassa and the Wondo Genet observed time series remained constant. It can be stated that precipitation can be excluded as source of the increase in discharge. This was concluded by Herder (2013) and Belete (2013) as well. This indicates modification of the hydro-system within the Tikur Woha subbasin.

The discharge increases of the Wosha and Tikur Woha streams are most likely related to land use changes within the Tikur Woha subbasin, especially to the increase in agricultural land use (Herder, 2013). The land use change can increase the surface runoff. Agricultural land that has been introduced in deforested areas has less interception of precipitation than natural forest. Runoff can be significant, especially after harvesting crops, compared to forest rich areas. This could support the increase in discharge of the Tikur Woha. Herder (2013) revealed a decrease in the actual evapotranspiration rate. She mentioned a relationship between the decrease in evapotranspiration and the increase in discharge. When evapotranspiration declines the soil water content increases. But the water holding capacity is limited and therefore the extra water contributes to streamflow which results into an increase in discharge.

The Tikur Woha discharge increase could also be a result of the decreasing swamps storage capacity (Gebreegziabher, 2004). The swamps surface area and thus its storage capacity is decreasing due to siltation and transition of swamp area into agricultural land use (Ayenew, 2004; Gebreegziabher, 2004; Ayenew et al., 2007; Shewangizaw and Michael, 2010; Belete, 2013).

Interesting is the effect of backwater on the Tikur Woha discharge. Ayenew and Gebreegziabher (2006) faced some model problems between the computed and observed levels of Lake Awassa. They stated that the Tikur Woha discharge measurements were affected by the backwater effect. The backwater effect can significantly affect the discharge measurements (Hidayat et al., 2011). Despite, the backwater effect is not taken into consideration in all known studies about the Awassa catchment. This could result into wrong interpretations.

The Tikur Woha discharge time series shows an enormous high base flow for the years 1996 to 2006, especially for the year 1998. Strangely, the peak flows in those year are not higher than average. The backwater effect could explain the high baseflow during those years. In the years 1996 to 2006 the Awassa lake level is above average as well. The water level in the Tikur Woha could rise parallel with the rise of the Awassa lake level. Since the discharge measurement station stands within a close radius from the river mouth the measurements are likely to be affected by the backwater effect. In 1998 the base flow is almost as high as an average peak flow. This can be related to the flooding due to the highest lake level in decades. The relationship between the lake level peaks for the years 1989 and 1990 and the high base flows supports the backwater effect theory. It is very likely that the increase in discharge is smaller than previously stated. However an increase in discharge is still likely due to the hydrology and land use changes in the Tikur Woha subbasin. In addition, the Awassa lake level is likely to be increase due to higher discharges.

5.2 Model performance

The model performance is statistically reviewed by consulting the Coefficient of determination (R^2), the Nash-Sutcliffe efficiency (NSE), and the percent bias (PBIAS). The mean observed flow during the calibration period is 2.91 m^3/s whereas the mean simulated flow is 2.94 m^3/s for the same period. The mean observed flow during the validation time series is 3.31 m^3/s whereas the mean simulated flow is 3.25 m^3/s. The average discharges in both calibration and validation results shows a very close similarity. Thus, the model can be used very well to predict the mean annual discharges. The R^2 value for calibration and validation is respectively 0.28 and 0.01. This indicates a high error variance in the model. The model can therefore not being used for determining peak flows with a high certainty. According to the Nash and Sutcliffe Efficiency (NSE) the model performs during the calibration period with 0.25 acceptable but unsatisfactory (Moriasi, 2007). However during the validation period the model performs accordingly to the NSE value of -0.43 not acceptable. The percent bias (PBIAS) has the ability to clearly indicate poor model performance (Gupta, 1999). The PBIAS value of -1.2 for calibration period indicates that the model slightly overestimates stream flow during this period. For the validation period however, the PBIAS value of 1.9 indicates model underestimation. This is in line with the earlier mentioned hypothesis. The PBIAS value reveals that the model simulation during the calibration period is slightly more accurate than the simulation during the validation period. Accordingly to the PBIAS rating the model performs during both calibration and validation good (PBIAS < 10%) (Moriasi, 2007). Overall the model performs acceptable, especially in predicting mean annual discharges. The model is during the calibration and validation period compared with the Tikur Woha discharge series that is affected by the backwater effect. A discharge data set without the backwater effect would very likely result into a better performance overall.

5.3 Irrigation abstraction

The limited number of discharge measurements and the short measurement period doesn't provide long-term information. However the measured data provides a useful insight in the abstraction due to irrigation. The measurement period (field work) was carried out at the end of the *Kiremt* and at the begin of the *Bega*, while the irrigation period is mainly during the complete *Bega* period. Even though the lack of irrigation data the auto-irrigation performed by SWAT is simulated well. Nevertheless, the simulated irrigation may still be underestimated.

Yearly, the mean monthly Wosha discharge simulated by the run with irrigation is 0.49 ± 0.25 m^3/s whereas the mean monthly simulated without irrigation is 0.52 ± 0.22 m^3/s. It may seems like a small

influence of irrigation on the Wosha hydrology but the decrease in discharge is significant for the months December, January and February ($p<0.01$). The decrease in discharge in those months is respectively -17.6 ± 13.5%, -26.0 ± 14.4% and -31.3 ± 18.6%. Yearly, the decrease in the Wosha discharge due to irrigation would be ± $0.93 \cdot 10^6$ m^3. The scale of abstraction due to irrigation is noticeable on catchment scale. Since the decrease in the Tikur Woha discharge due to irrigation would be ± $1.7 \cdot 10^6$ m^3 annually. Significant water abstractions follows in the months December, January and February ($p<0.01$). The decrease in discharge in those months is respectively -5.8 ± 4.2%, -9.8 ± 5.4% and -13.8 ± 7.7%.

Improvement in irrigation efficiency would reduce this water abstraction enormously. New concrete channels were built as a result of recent governmental projects. These projects haven't been taken into account. It is likely that the effects of recent projects are currently too little due to the scale of irrigation. Water abstractions in agricultural subbasins are very high, this already results in local discussions between farmers upstream and downstream. Farmers upstream divert stream water to their lands which results into less irrigation water downstream. At the moment, some small streams like the Worka, Hallo, Shonkora and Abosa are dried up before reaching the swamp. Hypothetically, the swamp water volume declines and the aquifer below the Tikur Woha subbasins can decrease in volume when extensive water will be pumped out of the aquifer. Furthermore the evapotranspiration can increase as a consequence of poor irrigation management. The evaporation is large at water filled basins, designed for irrigation purposes. All the evapotranspirated water is lost out of the Awassa catchment.

5.4 Swamp effect

Two scenarios have been simulated to quantify the effects of the swamp. In one scenario the area of the swamp has been replaced by agricultural fields (sugercane). The second scenario adds an irrigation scheme, of the same water abstraction rate as modelled for the crops in surrounding areas, to scenario one. It is highly likely that in the future the swamp area declines. Valuable swamp areas are claimed by local farmers which results in a transition from swamp into agricultural land use. The monthly mean simulated Tikur Woha discharge, with the swamp taken into account, is 2.71 ± 0.65 m^3/s. The monthly mean simulated Tikur Woha discharge, with irrigated sugercane fields, is 5.68 ± 4.54 m^3/s. The same simulated discharge series but without irrigation results into a mean monthly discharge of 5.95 ± 4.25 m^3/s. There is a huge difference in Tikur Woha discharge between both scenario simulations and the current situation. The difference between the current situation and the simulation scenarios without and with irrigation would be yearly in terms of water volume ± $102.2 \cdot 10^6$ m^3 and ± $93.7 \cdot 10^6$ m^3 respectively. The increase in mean discharge could be explained by evaporation and transpiration. The evaporation is currently high since water is stored in the swamp as open water, this results into a higher evaporation compared to unsaturated and saturated soils. If the swamp area decreases and makes place for agricultural land then it would be likely that the evaporated water volume decreases. The water volume would then likely contributes to the streamflow. This can explain the increase in the discharge of the Tikur Woha River.

It is very likely that there would be a change in the magnitude of the peak flows when the swamp disappears. The magnitude of discharge intensities from the no reservoirs simulation is enormously increased compared to the simulation with reservoirs. The swamps storage function would be inactive when the swamp itself disappears. It means that all runoff waters located upstream the swamp aren't buffered anymore. Peak flows of the eighth streams accumulate at the location of the current swamp.

The accumulated water may lead to flooding of high populated downstream area nearby the city Awassa. The discharge during the wet months increases significantly with values between 100 and 150% in both runs. During the *Bega* period the discharge increases significantly as well. However it is highly likely that the discharge difference would be less than predicted. Strangely the discharge simulated by the irrigated sugercane scenario increases more during the *Bega* period than the scenario without irrigation.

6. Conclusion

Both streamflow of the Wosha and Tikur Woha river significantly increased during the observed period from 1980 to 1996 and 1981 to 2006 respectively ($p<0.05$). The increase in the Tikur Woha discharge is found to be 0.064 m^3/s or $2.0 \cdot 10^6$ m^3 annually, which is 2.8 times higher than the Wosha discharge. The long-term significant increasing trend of discharge cannot be explained by precipitation changes, since the Awassa and the Wondo Genet observed time series remained constant.

The discharge increase of the Wosha and Tikur Woha streams are most likely related to land use changes within the Tikur Woha subbasin, especially to the increase in agricultural land use.

The backwater effect in the Tikur Woha significantly affects the discharge measurements due to high Awassa lake levels for the years 1989 and 1990 and for the period 1997-2006. Therefore can be stated that the increase in Tikur Woha discharge is very likely smaller than previously stated in other studies.

The average discharges simulated by the model show a very close similarity. Thus, the model can be used very well to predict the mean annual Wosha discharges. The Coefficient of Determination (R^2) for both calibration and validation are respectively 0.28 and 0.01. This indicates a high error variance in the model. The model can therefore not being used for determining peak flows with a high certainty. According to the Nash and Sutcliffe Efficiency (NSE) the model performs during the calibration period with 0.25 acceptable but unsatisfactory. However during the validation period the model performs with a NSE value of -0.43 not acceptable. According to the PBIAS rating the model performs during both calibration and validation very good. Overall the model performs acceptable, especially in predicting mean annual discharges. The model performs satisfactory when its complexity and the lack of detailed data with a low measurement error is taken into account. A discharge data set without the backwater effect would very likely result into a better performance overall.

The decrease in discharge due to irrigation abstractions is significant for the months December, January and February ($p<0.01$). The decrease in discharge in those months is respectively -17.6 ± 13.5%, -26.0 ± 14.4% and -31.3 ± 18.6%. Yearly, the decrease in the Wosha discharge due to irrigation would be ± $0.93 \cdot 10^6$ m^3.

The irrigation in the Awassa catchments has an intermediate effect on the total streamflow of the Tikur Woha River. Yearly, the decrease in the Tikur Woha discharge due to irrigation would be ± $1.7 \cdot 10^6$ m^3. Significant water abstractions follows in the months December, January and February ($p<0.01$). The decrease in discharge in those months is respectively -5.8 ± 4.2%, -9.8 ± 5.4% and -13.8 ± 7.7%.

The swamp has a significant effect on the water balance in the Tikur Woha subbasin. The discharge during the wet months increases significantly with values between 100 and 150% in the two simulations. The monthly mean simulated Tikur Woha discharge, with the swamp taken into account, is 2.71 ± 0.65 m3/s. The monthly mean simulated Tikur Woha discharge, with irrigated sugarcane fields, is 5.68 ± 4.54 m3/s. The same simulated discharge series but without irrigation results into a mean monthly discharge of 5.95 ± 4.25 m3/s.

The difference between the current situation and the simulation scenarios without and with irrigation would be yearly in terms of water volume ± $102.2 \cdot 10^6$ m^3 and ± $93.7 \cdot 10^6$ m^3 respectively. The increase in mean discharge could be explained by evaporation. It is very likely that the open water evaporation decreases which results into a higher Tikur Woha discharge.

Furthermore, the swamp area retains high peak discharges from the upstream area. Future cultivation of the swamp area may lead to flooding of high populated downstream area.

7. List of references

ABBASPOUR, K. C., ROUHOLAHNEJAD, E., VAGHEFI, S., SRINIVASAN, R., YANG, H. & KLØVE, B. 2015a. Building an Agro-Hydrologic Model of Europe: Model Calibration Issues. 21st International Congress on Modelling and Simulation.

ABBASPOUR, K. C., ROUHOLAHNEJAD, E., VAGHEFI, S., SRINIVASAN, R., YANG, H. & KLØVE, B. 2015b. Continental-scale hydrology and water quality model for Europe: Calibration and uncertainty of a high-resolution large-scale SWAT model. *Journal of Hydrology,* 524**,** 733-752.

ABTEW, W., MELESSE, A. M. & DESSALEGNE, T. 2009. El Niño Southern Oscillation link to the Blue Nile River Basin hydrology. *Hydrological Processes,* 23**,** 3653-3660.

ACHAMYELEH, K. 2003. Case Study - Ethiopia: Intergrated Flood Management. *THE ASSOCIATED PROGRAMME ON FLOOD MANAGEMENT.*

AHMAD, M., ALI, B., ALI, S., ASLAM, M., BABAR, Q. R., HAIDER, M. S., HUSSEIN, K., LFTIKHAR, S., LQBAL, A., KHAN, M. A., KUPER, M., MEHMOOD, L., PASHA, M. A., RAMZAN, M., RAZA, F. A., RAZAQ, A., RIAZ, A., SAMAD, A., SHAH, Q. A., SHAUQ, G. R. & SKOGERBOE, G. 1995. Field Calibration of Irrigation Flow Control Structures.

ALEMAYEHU ABIYE, T. 2008. Environmental resources and recent impacts in the Awassa collapsed caldera, Main Ethiopian Rift. *Quaternary International,* 189**,** 152-162.

ARNOLD, J. G., SRINIVASAN, R., MUTTIAH, R. S. & WILLIAMS, J. R. 1998. LARGE AREA HYDROLOGIC MODELING AND ASSESSMENT PART I: MODEL DEVELOPMENT1. *JAWRA Journal of the American Water Resources Association,* 34**,** 73-89.

ASHAGRIE, Y. & ZECH, W. 2010. Water and nutrient inputs in rainfall into natural and managed forest ecosystems in south-eastern highlands of Ethiopia. *Ecohydrology & Hydrobiology,* 10**,** 169-181.

AYENEW, T. 2004. Environmental implications of changes in the levels of lakes in the Ethiopian Rift since 1970. *Regional Environmental Change,* 4**,** 192-204.

AYENEW, T. 2007. Water management problems in the Ethiopian rift: Challenges for development. *Journal of African Earth Sciences,* 48**,** 222-236.

AYENEW, T., BECHT, R., LIESHOUT, A. V., GEBREEGZIABHER, Y., LEGESSE, D. & ONYANDO, J. 2007. Hydrodynamics of topographically closed lakes in the Ethio-Kenyan Rift: The case of lakes Awassa and Naivasha. *Journal of Spatial Hydrology,* 7**,** 81-100.

AYENEW, T., DEMLIE, M. & WOHNLICH, S. 2008. Hydrogeological framework and occurrence of groundwater in the Ethiopian aquifers. *Journal of African Earth Sciences,* 52**,** 97-113.

AYENEW, T. & GEBREEGZIABHER, Y. 2006. Application of a spreadsheet hydrological model for computing the long-term water balance of Lake Awassa, Ethiopia. *Hydrological Sciences Journal,* 51**,** 418-431.

BELETE, M. D. 2013. *The impact of sedimentation and climate variability on the hydrological status of Lake Hawassa, South Ethiopia.* PhD, Rheinischen Friedrich-Wilhelms-University Bonn.

BELETE, M. D., DIEKKRÜGER, B. & ROEHRIG, J. 2015. Characterization of Water Level Variability of the Main Ethiopian Rift Valley Lakes. *Hydrology,* 3.

BEWKET, W. & STERK, G. 2005. Dynamics in land cover and its effect on stream flow in the Chemoga watershed, Blue Nile basin, Ethiopia. *HYDROLOGICAL PROCESSES,* 19**,** 445–458.

BROUWER, C., PRINS, K. & HEIBLOEM, M. 1989. Irrigation Water Management: Irrigation Scheduling: Training manual no. 4.

CHEUNG, W. H., SENAY, G. B. & SINGHA, A. 2008. Trends and spatial distribution of annual and seasonal rainfall in Ethiopia. *INTERNATIONAL JOURNAL OF CLIMATOLOGY,* 28**,** 1723–1734.

CHOROWICZ, J. 2005. The East African rift system. *Journal of African Earth Sciences,* 43**,** 379-410.

CORTI, G. 2009. Continental rift evolution: From rift initiation to incipient break-up in the Main Ethiopian Rift, East Africa. *Earth-Science Reviews,* 96**,** 1-53.

DEGEN 2016. MSc Research

DESSIE, G. & KLEMAN, J. 2007. Pattern and Magnitude of Deforestation in the South Central Rift Valley Region of Ethiopia. *Mountain Research and Development,* 27**,** 162–168.

DILE, Y. T. & SRINIVASAN, R. 2014. Evaluation of CFSR climate data for hydrologic prediction in data-scarce watersheds: an application in the Blue Nile River Basin. *JAWRA Journal of the American Water Resources Association,* 50**,** 1226-1241.

DUBE, E., CHIDUZA, C. & MUCHAONYERWA, P. 2012. Conservation agriculture effects on soil organic matter on a Haplic Cambisol after four years of maize–oat and maize–grazing vetch rotations in South Africa. *Soil and Tillage Research,* 123**,** 21-28.

FISCHER, G., F. NACHTERGAELE, S. PRIELER, H.T. VAN VELTHUIZEN, L. VERELST, D. WIBERG, 2008. Global Agro-ecological Zones Assessment for Agriculture (GAEZ 2008). *IIASA*.

FUKA, D. R., WALTER, M. T., MACALISTER, C., DEGAETANO, A. T., STEENHUIS, T. S. & EASTON, Z. M. 2014. Using the Climate Forecast System Reanalysis as weather input data for watershed models. *Hydrological Processes,* 28**,** 5613-5623.

GEBREEGZIABHER, Y. 2004. *Assessment of the Water Balance of Lake Awassa Catchment, Ethiopia.* MSc Thesis, International Institute for Geo-Information Science and Earth Observation

GRIENSVEN, A. V., NDOMBA, P., YALEW, S. & KILONZO, F. 2012. Critical review of SWAT applications in the upper Nile basin countries. *Hydrol. Earth Syst. Sci.,* 16**,** 3371–3381.

GUPTA, H. V., S. SOROOSHIAN, P.O. YAPO 1999. Status of automatic calibration for hydrologic models: Comparison with multilevel expert calibration. *J.Hydrologic Eng.,* 4**,** 135-143.

HASSAN, A. A. & JIN, S. 2014. Lake level change and total water discharge in East Africa Rift Valley from satellite-based observations. *Global and Planetary Change,* 117**,** 79-90.

HENGSDIJK, H. & JANSEN, H. 2006. Agricultural development in the Central Ethiopian Rift valley: A desk-study on water-related issues and knowledge to support a policy dialogue. *Plant Research International B.V.,* Note 375.

HERDER, C. 2013. *Impacts of land use changes on the hydrology of Wondo Genet catchment in Ethiopia.* MSc Thesis, Utrecht University.

HIDAYAT, H., VERMEULEN, B., SASSI, M. G., TORFS, P. J. J. F. & HOITINK, A. J. F. 2011. Discharge estimation in a backwater affected meandering river. *Hydrol. Earth Syst. Sci.,* 15**,** 2717-2728.

HOLMES, J., R.R., TERRIO, P.J., HARRIS, M.A., AND MILLS, P.C. 2001. Introduction to Field Methods for Hydrologic and Environmental Studies.

J. G. ARNOLD, D. N. M., P. W. GASSMAN, K. C. ABBASPOUR, M. J. WHITE,, R. SRINIVASAN, C. S., R. D. HARMEL, A. VAN GRIENSVEN, & M. W. VAN LIEW, N. K., M. K. JHA 2012. SWAT: Model Use, Calibration, and Validation. *American Society of Agricultural and Biological Engineers,* 55**,** 1491-1508.

KORECHA, D. & BARNSTON, A. G. 2007. Predictability of June–September Rainfall in Ethiopia. *Monthly Weather Review,* 135**,** 628-650.

KUUSISTO, E. 1996. *Water Quality Monitoring - A Practical Guide to the Design and Implementation of Freshwater Quality Studies and Monitoring Programmes*, United Nations Environment Programme, World Health Organization.

LIERSCH, S. 2003a. Program a: pcpSTAT. Berlin.

LIERSCH, S. 2003b. Program b: dew02. Berlin.

MACGREGOR, D. 2015. History of the development of the East African Rift System: A series of interpreted maps through time. *Journal of African Earth Sciences,* 101**,** 232-252.

MORIASI, D. N., ARNOLD, J.G. , VAN LIEW, M.W. , BINGNER, R.L. , HARMEL, R.D. , VEITH, T.L. 2007. Model evaluation guidelines for systematic quantification of accuracy in watershed simulations. *American Society of Agricultural and Biological Engineers,* 50**,** 885-900.

NASH, J. E. & SUTCLIFFE, J. V. 1970. River Flow Forecasting through Conceptual Models 1. A Discussion of Principles. *Journal of Hydrology,* 10**,** 282-290.

NEITSCH, S. L., ARNOLD, J. G., KINIRY, J. R. & WILLIAMS, J. R. 2011. Soil and Water Assessment Tool – Theoretical Documentation Version 2009. Texas, USA: Texas A&M University

OVERTON, D. E. 1966. Muskingum flood routing of upland streamflow. *Journal of Hydrology,* 4**,** 185-200.

PENMAN, H. L. 1956. Evaporation: An introductory survey. *Netherlands Journal of Agricultural Science,* 4**,** 7-29.

REYNOLDS, T. W., FARLEY, J. & HUBER, C. 2010. Investing in human and natural capital: An alternative paradigm for sustainable development in Awassa, Ethiopia. *Ecological Economics,* 69**,** 2140-2150.

SAXTON, K. E. 2007. Soil Water Characteristics. *In:* SERVICE, U. A. R. (ed.) 6.02.74 ed.

SELESHI, Y. & ZANKE, U. 2004. Recent changes in rainfall and rainy days in Ethiopia. *International Journal of Climatology,* 24**,** 973-983.

SHEDD, J. R. 2011. Standard Operating Procedure for Measuring and Calculating Stream Discharge. *In:* ECOLOGY, W. S. D. O. (ed.) *Environmental Assessment Program.*

SHEWANGIZAW, D. & MICHAEL, Y. 2010. Assessing the Effect of Land Use Change on the Hydraulic Regime of Lake Awassa. *Nile Basin Water Science& Engineering Journal,* 3**,** 110-118.

SLOAN, P. G., MORRE, I. D., COLTHARP, G. B. & EIGEL, J. D. 1983. Modeling surface and subsurface stormflow on steeply-sloping forested watersheds. *Water Resources Inst. Report 142.* University Kentucky, Lexington.

SRINIVASAN, R. 2013. *Custom Weather Generator: RAINHHMX (Maximum 0.5 h rainfall) Problem* [Online]. Google Groups: SWAT-user. Available: https://groups.google.com/forum/#!topic/swatuser/kpZMCke3BvU.

TEKLAY, T., NORDGREN, A. & MALMER, A. 2006. Soil respiration characteristics of tropical soils from agricultural and forestry land-uses at Wondo Genet (Ethiopia) in response to C, N and P amendments. *Soil Biology and Biochemistry,* 38**,** 125-133.

TEMESGEN, H., NYSSEN, J., ZENEBE, A., HAREGEWEYN, N., KINDU, M., LEMENIH, M. & HAILE, M. 2013. Ecological succession and land use changes in a lake retreat area (Main Ethiopian Rift Valley). *Journal of Arid Environments,* 91**,** 53-60.

TURNIPSEED, D. P. & SAUER, V. B. 2010. *Discharge Measurements at Gaging Stations*.

WOLKA, K., TADESSE, H., GAREDEW, E. & YIMER, F. 2015. Soil erosion risk assessment in the Chaleleka wetland watershed, Central Rift Valley of Ethiopia. *Environmental Systems Research,* 4**,** 1-12.

ŽÁČEK V., R. V., AMAN Y., BERHANU B., ČÍŽEK D., DEREJE K., ERBAN V., EZRA T., FIRDAWOK L., HABTAMU M., HROCH T., KOPAČKOVÁ V., MÁLEK J., MALÍK J., MIŠUREC J., ORGOŇ A., PÉCSKAY Z., ŠÍMA J., TAREKEGU D., VERNER K. 2014a. Explanation booklet to the Set of Geoscience maps of Ethiopia at a scale 1 : 50,000: sub-sheet 0738-C4 Hawassa. *Geological Survey of Ethiopia (GSE).*

ŽÁČEK V., R. V., AMAN Y., BERHANU B., ČÍŽEK D., DEREJE K., ERBAN V., EZRA T., FIRDAWOK L., HABTAMU M., HROCH T., KOPAČKOVÁ V., MÁLEK J., MALÍK J., MIŠUREC J., ORGOŇ A., PÉCSKAY Z., ŠÍMA J., TAREKEGU D., VERNER K. 2014b. Explanation booklet to the Set of Geoscience maps of Ethiopia at a scale 1 : 50,000: sub-sheet 0738-D3 Shashemene. *Geological Survey of Ethiopia (GSE).*

ZEMADIM, B. & SCHMIDT, E. 2013. Understanding impacts of sustainable land management interventions using SWAT Hydrological Model. Addis Ababa, Ethiopia: Nile Basin Development Challenge (NBDC) Science Workshop.

8. Appendices

8.1 Location weather stations.

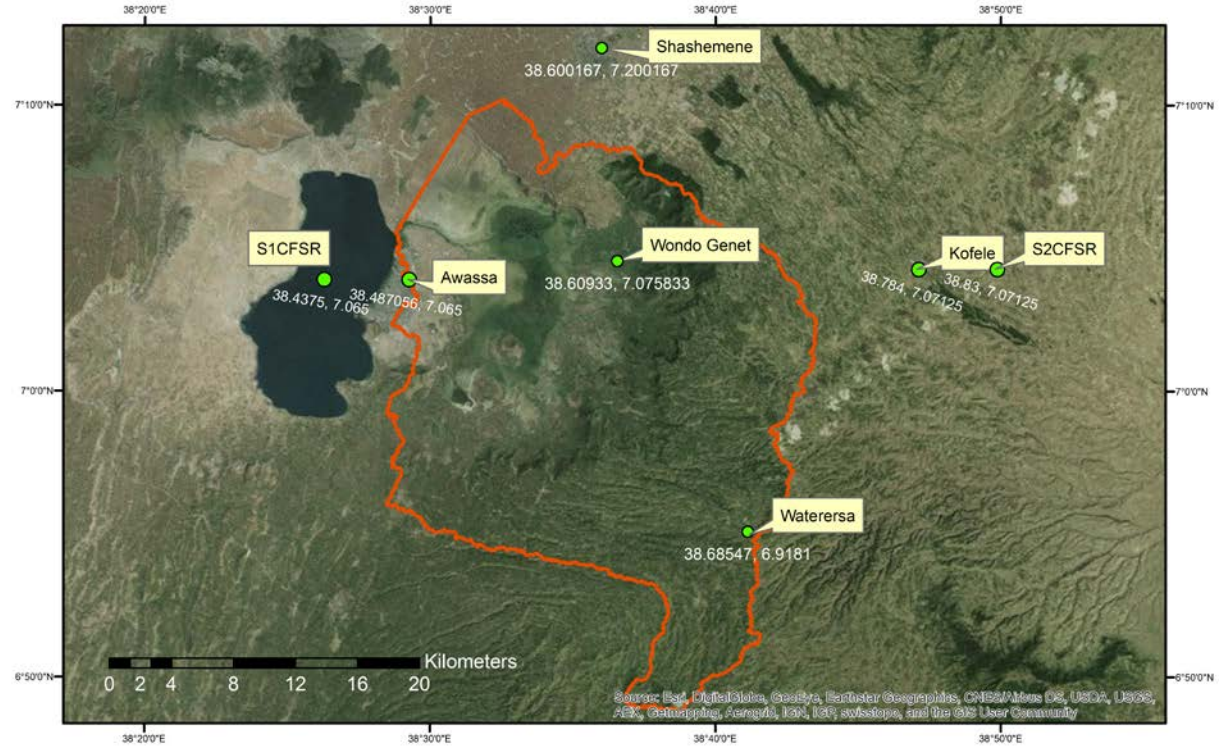

Figure 20: Location of used weather stations.

8.2 Location flow velocity measurement points.

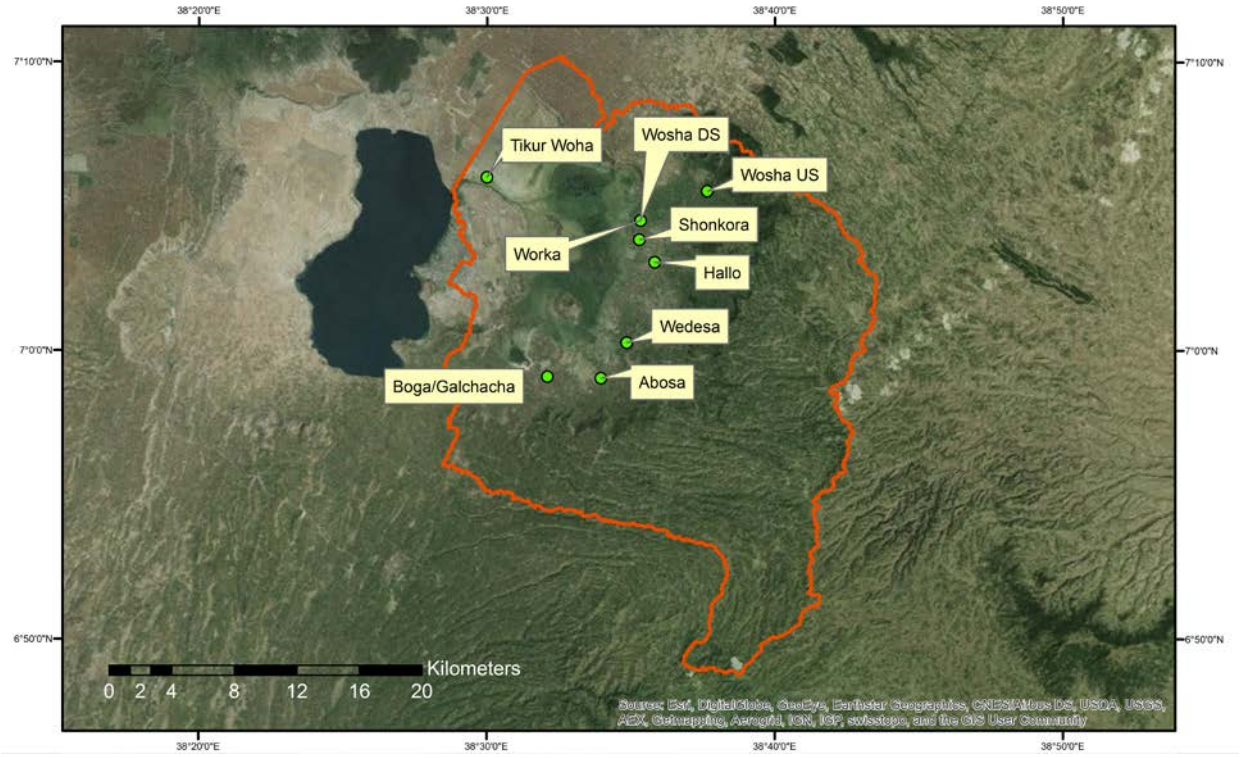

Figure 21: Location of the discharge measurement sites.

8.3 Digital elevation model

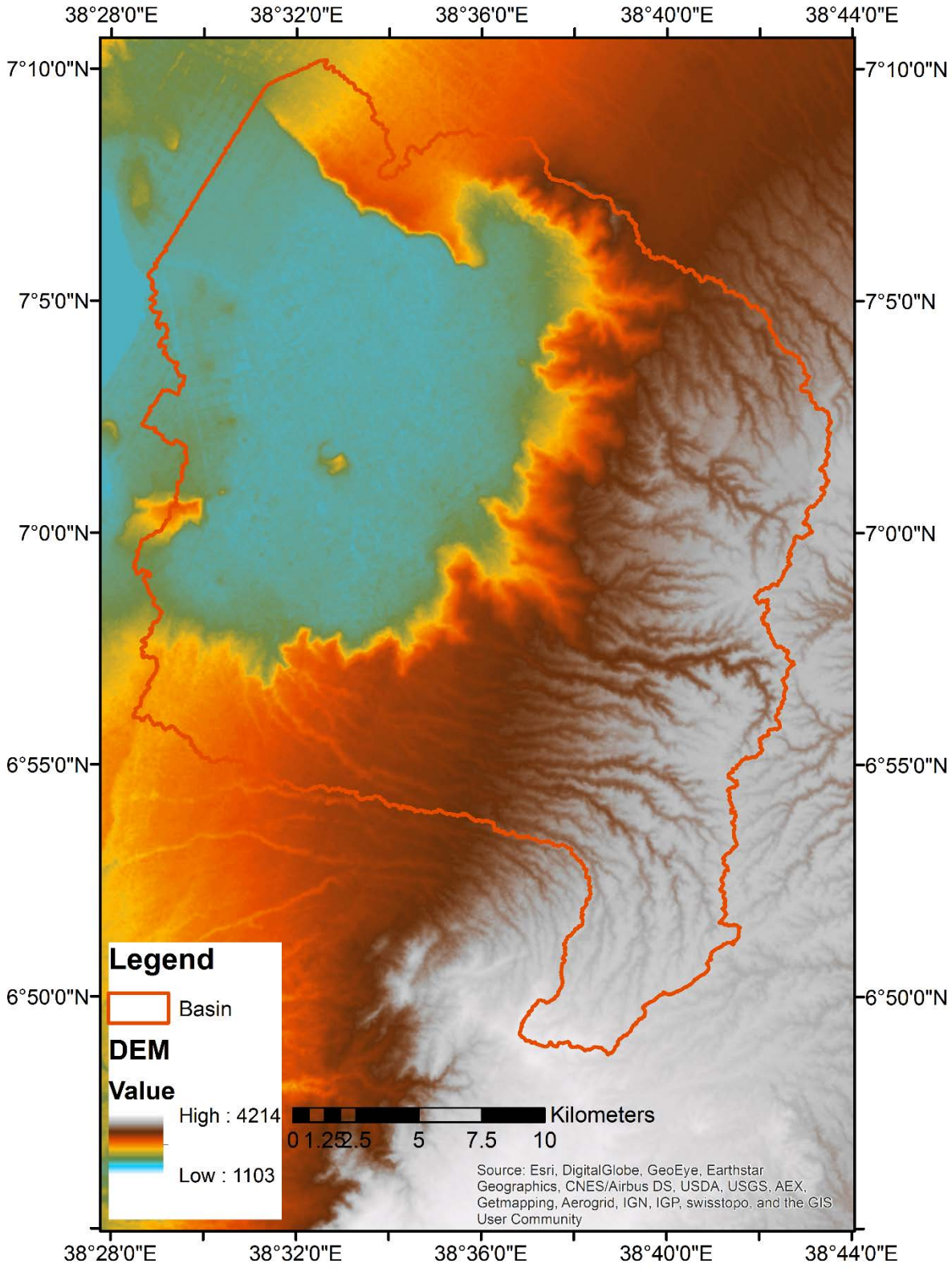

Figure 22: Digital elevation model of the Tikur Woha subbasin.

8.4 Soil class map

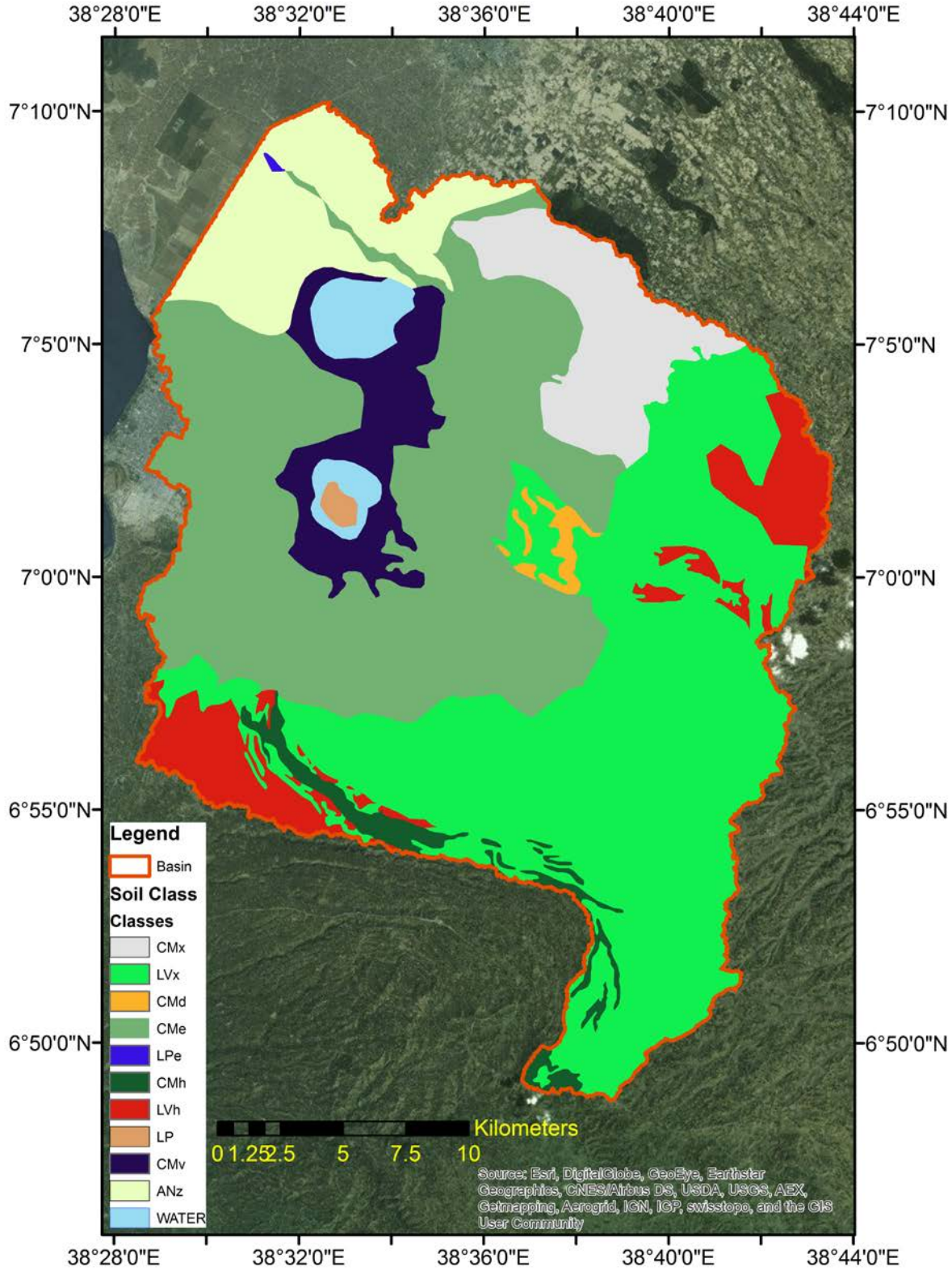

Figure 23: Soil map created by The Rift Valley Lakes Basin Integrated Resources Development Master Plan Study Project.

8.5 Land use map

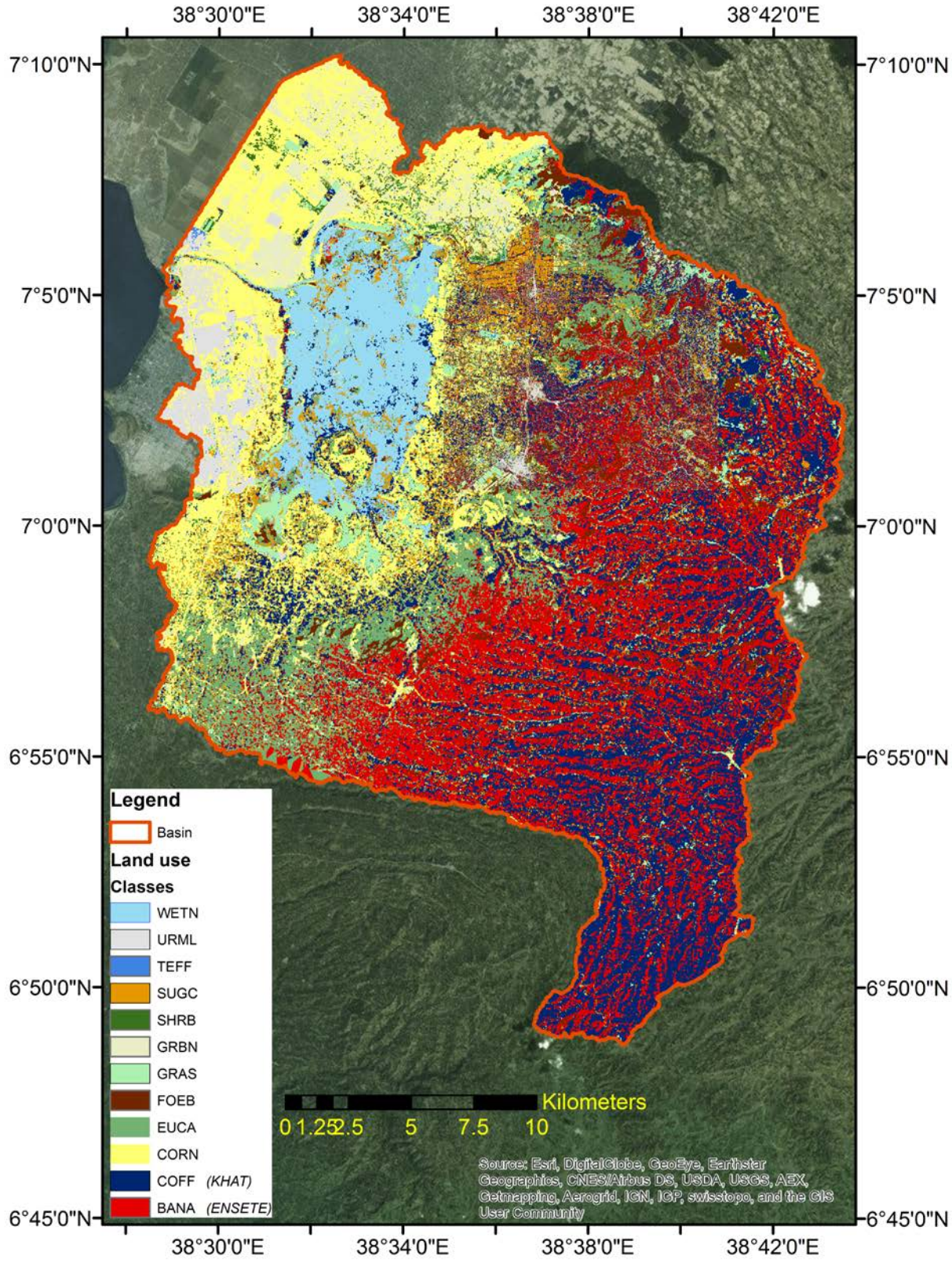

Figure 24: Land use map developed by Degen (2016)

8.6 Land slope map

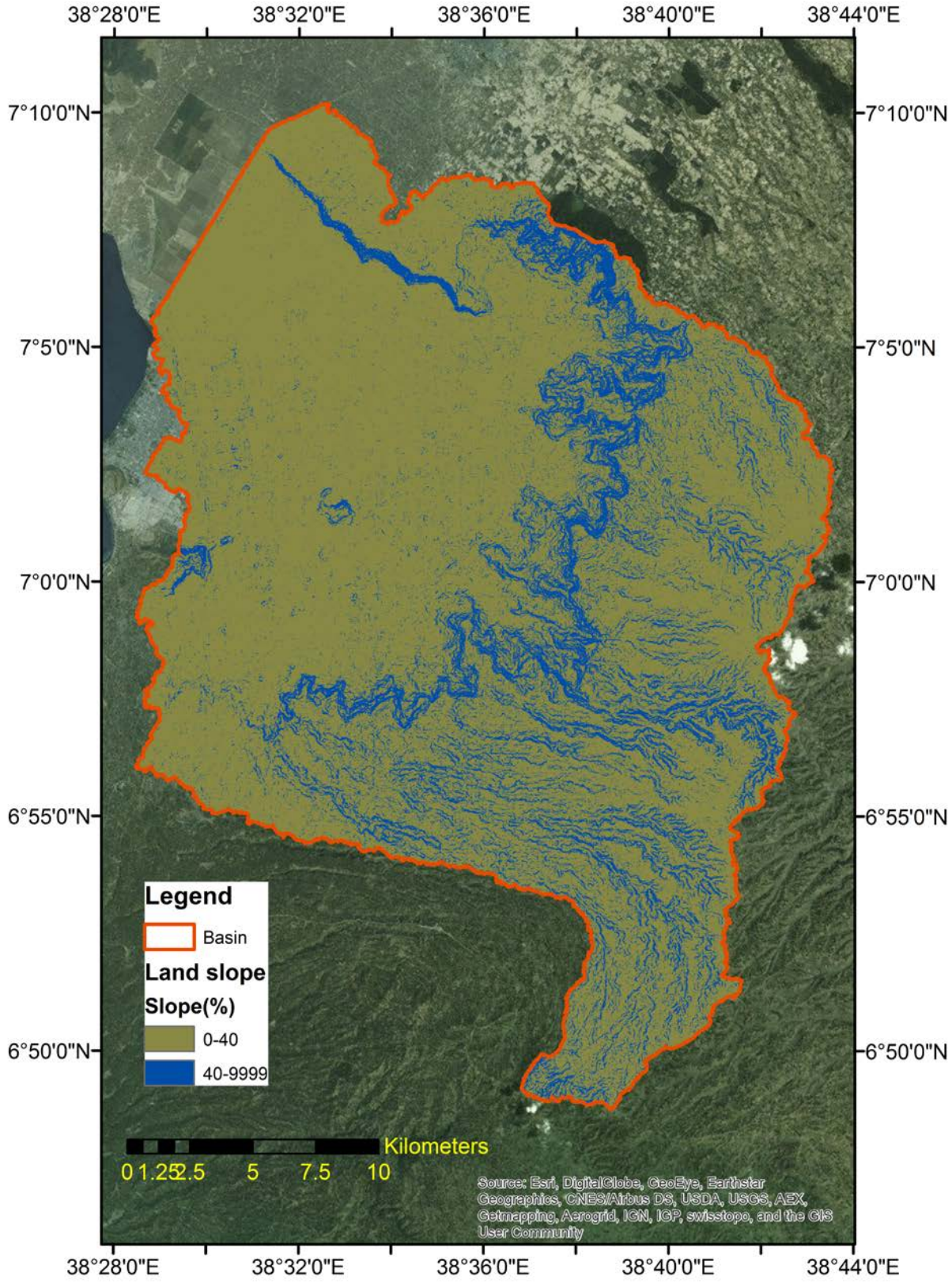

Figure 25: Land slope map produced by the SWAT programme.

8.7 SWAT model

8.7.1 Parameterization

Table 2: Six most sensitive parameters in the first Wosha subbasin modelling stage.

Parameter	Description	[Unit]	Recommended SWAT range	Calibrated value
CN2	Curve number for the moisture condition II	[-]	35-98	**-5.29%**
SOL_AWC	Available water capacity in the soil	[mm/mm]	0-1	**-63.64%**
ESCO	Soil evaporation compensation factor	[-]	0-1	**0.96**
GW_DELAY	Groundwater delay	[Days]	0-500	**104.68**
GWQMN	Threshold depth of water in the shallow aquifer required for return flow to occur	[mm]	0-5000	**677.30**
ALPHA_BF	Baseflow alpha factor	[Days]	0-1	**0.0038**

Table 3: The five most sensitive reservoir parameters.

Parameter	Description	[Unit]	Recommended SWAT range	Calibrated value
RES_K	Hydraulic conductivity of the reservoir bottom	[mm/hr]	0-1	**0.29**
OFLOWMN	Minimum daily outflow data for the month	[m^3/s]	0-1000	**0.70**
OFLOWMX	Maximum daily outflow data for the month	[m^3/s]	0-2000	**1.35**
EVRSV	Lake evaporation coefficient	[-]	0-1	**0.64**
RES_RR	Average daily principal spillway release rate	[m^3/s]	0-1000	**1.64**

Table 4: The five most sensitive parameters of the remaining uncalibrated areas (Awassa calibration (Fig. 7)).

Parameter	Description	[Unit]	Recommended SWAT range	Calibrated value
CN2	Curve number for the moisture condition II	[-]	35-98	**-0.37%**

SOL_AWC	Available water capacity in the soil	[mm/mm]	0-1	**-29.29%**
GWQMN	Threshold depth of water in the shallow aquifer required for return flow to occur	[mm]	0-5000	**952.86**
GW_REVAP	Groundwater "revap" coefficient	[-]	0.02-0.2	**0.70**
REVAPMN	Threshold depth of water in the shallow aquifer for "revap" to occur	[mm]	0-500	**424.29**

8.7.2 Calibration and Validation

Table 5: Results of both Wosha subbasin calibration and validation.

Coefficient	**Calibration period (1987-1992)**		**Validation period (1993-1996)**	
	Sim. Flow [m^3/s]	**Obs. Flow [m^3/s]**	**Sim. Flow [m^3/s]**	**Obs. Flow [m^3/s]**
Mean	0.72	0.73	0.70	0.72
R^2	0.29		0.05	
NSE	0.29		0.00	
PBIAS	0.7		3.5	

Table 6: Results of the reservoir calibration.

Coefficient	**Calibration period (1987-2001)**		**Validation period (2002-2006)**	
	Sim. Flow [m^3/s]	**Obs. Flow [m^3/s]**	**Sim. Flow [m^3/s]**	**Obs. Flow [m^3/s]**
Mean	2.95	2.91	2.96	3.31
R^2	0.24		0.01	
NSE	0.22		-0.18	
PBIAS	-1.4		10.5	

Table 7: Results of simulated versus observed average monthly streamflow data.

Coefficient	Calibration period (1987-2001)		Validation period (2002-2006)	
	Sim. Flow [m^3/s]	Obs. Flow [m^3/s]	Sim. Flow [m^3/s]	Obs. Flow [m^3/s]
Mean	2.94	2.91	3.25	3.31
R^2	0.28		0.01	
NSE	0.25		-0.43	
PBIAS	-1.2		1.9	

8.7.3 Model performance

The hydrological SWAT model that was created has been calibrated and validated. The general model (Awassa calibration) was calibrate d by using measured Tikur Woha discharge data to adjust model parameters within realistic margins to reduce the uncertainty associated with SWATs prediction. Both Tikur Woha and Wosha discharge data show a long term significant increasing trend. This affected the statistical evaluation between the calibration and validation period since the model output doesn't show an increase in discharge. The simulated and observed discharge would differ more and more over time which would result into a far better calibration than validation performance. For example the calibration of the Wosha subbasin showed during testing phase a Coefficient of Determination (R^2) of 0.71 and a Nash and Sutcliffe Efficiency (NSE) of 0.71, which indicates a very good model performance. However, during the validation the model performance showed a poor NSE of -1.05 and a R^2 of 0.35. In this study the observed data has been ranked based on annual average discharge intensity to obtain a more average model outcome. This hypothetically means slightly discharge overestimation during the calibration period and slightly discharge underestimation during the validation period.

The model performance is statistically reviewed by consulting the Coefficient of determination (R^2), the Nash-Sutcliffe efficiency (NSE), and the percent bias (PBIAS). The mean observed flow during the calibration period is 2.91 m^3/s whereas the mean simulated flow is 2.94 m^3/s for the same period. The mean observed flow during the validation time series is 3.31 m^3/s whereas the mean simulated flow is 3.25 m^3/s. The average discharges in both calibration and validation results shows a very close similarity. Thus, the model can be used very well to predict the mean annual discharges. The R^2 value for calibration and validation is respectively 0.28 and 0.01. This indicates a high error variance in the model. The model can therefore not being used for determining peak flows with a high certainty. According to the Nash and Sutcliffe Efficiency (NSE) the model performs during the calibration period with 0.25 acceptable but unsatisfactory (Moriasi, 2007). However during the validation period the model performs accordingly to the NSE value of -0.43 not acceptable. The percent bias (PBIAS) has the ability to clearly indicate poor model performance (Gupta, 1999). The PBIAS value of -1.2 for calibration period indicates that the model slightly overestimates stream flow during this period. For the validation period however, the PBIAS value of 1.9 indicates model underestimation. This is in line with the earlier mentioned hypothesis. The PBIAS value reveals that the model simulation during the calibration period is slightly more accurate than the simulation during the validation period.

Accordingly to the PBIAS rating the model performs during both calibration and validation good (PBIAS < 10%) (Moriasi, 2007). Overall the model performs acceptable, especially in predicting mean annual discharges. The model performs satisfactory when its complexity and the lack of detailed data with a low measurement error is taken into account.

8.8 Data review

In this study the lack of data was present. For example, detailed plant characteristics of the crops khat and ensete were not known. Water amounts from springs or abstractions due to domestic water supply have not been quantified. Furthermore no long-term irrigation measurements were available. Apart from missing data, the available data could have been measured with a high measurement error. Some of the weather stations within the Lake Awassa catchment have been poorly maintained. For example the grass surrounding the weather instruments was not shortly cut and wildlife such as monkeys could easily influence the measurements. Furthermore buildings or trees are standing to close around the weather station, especially at the Awassa station. Buildings surrounding the weather station reduce the measured wind speed. In addition, the float method that has been used by the Ethiopian Ministry of Water, Irrigation & Energy to estimate the Wosha discharge is not nearly as accurate as the discharge measurements performed by the Aqua Data SENSA RC2 Water Velocity Meter.